Space Programs Summary No. 37-30, Volume VI

for the period September 1, 1964 to October 31, 1964

Space Exploration Programs and Space Sciences

JPL
JET PROPULSION LABORATORY
CALIFORNIA INSTITUTE OF TECHNOLOGY
PASADENA, CALIFORNIA

November 30, 1964

Space Programs Summary No. 37-30, Volume VI

for the period September 1, 1964 to October 31, 1964

Space Exploration Programs and Space Sciences

JET PROPULSION LABORATORY
CALIFORNIA INSTITUTE OF TECHNOLOGY
PASADENA, CALIFORNIA

November 30, 1964

Preface

The *Space Programs Summary* is a six volume, bimonthly publication designed to report on JPL space exploration programs, and related supporting research and advanced development projects. The subtitles of all volumes of the *Space Programs Summary* are:

Vol. I. The Lunar Program (Confidential)

Vol. II. The Planetary–Interplanetary Program (Confidential)

Vol. III. The Deep Space Network (Unclassified)

Vol. IV. Supporting Research and Advanced Development (Unclassified)

Vol. V. Supporting Research and Advanced Development (Confidential)

Vol. VI. Space Exploration Programs and Space Sciences (Unclassified)

The *Space Programs Summary,* Volume VI consists of an unclassified digest of appropriate material from Volumes I, II, and III and a reprint of the space science instrumentation studies of Volumes I and II. This instrumentation work is conducted by the JPL Space Sciences Division and also by individuals of various colleges, universities, and other organizations. All such projects are supported by the Laboratory and are concerned with the development of instruments for use in the NASA space flight programs.

W. H. Pickering

W. H. Pickering, *Director*
Jet Propulsion Laboratory

Space Programs Summary No. 37-30, Volume VI

Prepared under Contract No. NAS 7-100, National Aeronautics & Space Administration

Contents

BLANK PAGE

LUNAR PROGRAM

I. *Ranger* Project

A. Introduction

The *Ranger* Project was established to develop a space flight technology for transporting engineering and scientific instruments to the Moon and planets. Nine *Ranger* launchings, using *Atlas D–Agena B* vehicles, are now planned; seven of these flights have been made.

Rangers 1 and *2* (Block I) were not lunar-oriented, but were engineering evaluation flights to test the basic systems to be employed in later lunar and planetary missions. Several scientific experiments were carried on a non-interference basis. Both spacecraft performed satisfactorily within the constraints of the obtained satellite orbit. *Rangers 3, 4,* and *5* (Block II) carried a gamma-ray instrument, a TV camera, and a rough-landing seismometer capsule; all three of these flights experienced failures.

The objective of the *Ranger* Block III (*Rangers 6* through *9*) flights is to obtain pictures of the lunar surface, at least an order of magnitude better than those obtainable with Earth-based photography, which will be of benefit to both the scientific program and the U.S. manned lunar flight program. The *Ranger 6* spacecraft, which was launched from Cape Kennedy, Florida, on January 30, 1964, and impacted the Moon essentially on target on February 2, 1964, did not accomplish the primary flight objective due to a failure of the TV subsystem to transmit pictures. An extensive analysis of the TV subsystem failure was conducted, new and reworked hardware was assembled as the *Ranger 7* TV subsystem, and extensive testing of the reassembled TV subsystem was performed. The *Ranger 7* spacecraft was launched from Cape Kennedy, Florida, on July 28, 1964, and impacted the Moon on target on July 31, 1964. The mission flight objective was accomplished. The outstanding events of the mission were the precision of the trajectory correction and the transmission of 4304 video pictures of the lunar surface.

The updating operations and scheduled tests for the *Ranger* proof test model (PTM) were completed. The PTM will be maintained in the *Ranger 8* and *9* configuration for use in evaluating any problems that might develop during these missions. *Rangers 8* and *9* are in various stages of assembly; subsystem and system tests are being performed.

B. Investigation of *Ranger* Launch-to-Injection Environment

Subsequent to the *Ranger 6* flight, questions were raised regarding the possible effects of the launch vehicle and the launch-to-injection environment upon the operation of the spacecraft. Investigations were started in the areas of electrical transients, accumulated high electrostatic charges, mechanical and electrical operations of the umbilical plug and door, ionized gases, and blast waves at booster ejection. It was intended to determine through these investigations: (1) whether this environment could have affected the operation of the *Ranger 6* TV circuits, and (2) whether the changes introduced on the *Ranger 7* spacecraft would preclude any deleterious effects because of the above-mentioned phenomena.

Extensive analyses and tests of *Ranger* spacecraft susceptibility to high-voltage charge and discharge transients were performed to determine whether charging of the spacecraft and launch vehicle due to the rocket engines, or subsequent discharge of a charged vehicle to clouds or exhaust trail, could create a mechanism for spacecraft degradation or failure. Since the shroud around the spacecraft is not a perfect conducting surface, some field will exist inside it and will be available to induce voltage into spacecraft circuitry. Spacecraft thermal-control-model tests were conducted to determine the magnitude of induced transients into typical spacecraft circuitry and to evaluate the possibility of these transients as failure-producing effects. Although the transients yielded during the tests were not of sufficient magnitude to constitute a probable cause of "catastrophic" failure, the possibility did exist of a temporary malfunction of a live spacecraft. As a result, the proof test model (PTM) in the *Ranger 7* configuration was also subjected to this high-voltage environment. No temporary or permanent malfunction or failure occurred on the PTM during these tests.

Some umbilical lines were shown to be sensitive to electrical transients during tests of the PTM in the *Ranger 7* electrical configuration, but no anomalies similar to the *Ranger 6* events were noted.

One recommendation resulting from the investigations thus far is that launch vehicles be instrumented to provide actual and accurate flight data in order to better understand the flight environment and more specifically determine the electrostatic charging and discharging rates. Investigations of the suspected potential problem areas will continue.

C. *Ranger 7* Trajectory Analysis

Launch phase. The *Ranger 7* spacecraft was launched at 16:50:07:873 GMT on July 28, 1964, from the Air Force Eastern Test Range at Cape Kennedy, Florida, using an *Atlas D–Agena B* boost vehicle. The inertial launch azimuth was 96.6 deg east of north. After liftoff, the booster rolled to an azimuth of 97.1 deg and performed a programmed pitch maneuver until booster cutoff. During the sustainer and vernier stages, adjustments in vehicle attitude and engine cutoff times were commanded as required by the ground guidance computer to adjust the altitude and velocity at *Atlas* vernier engine cutoff. After *Atlas–Agena* separation, there was a short coast period prior to the first ignition of the *Agena* engine. At a preset value of sensed velocity increase, the *Agena* engine was cut off. At this time the *Agena*–spacecraft combination was coasting in a nearly circular parking orbit in a southeasterly direction at an altitude of 188 km and an inertial speed of 7.80 km/sec. After an orbit coast time of 19.97 min, as determined by the ground guidance computer and transmitted to the *Agena* during the *Atlas* vernier stage, a second ignition of the *Agena* engine occurred. 89 sec later, the *Agena* was cut off with the *Agena*–spacecraft combination in a nominal Earth–Moon transfer orbit. The launch-phase ascent trajectory profile is illustrated in Fig. 1; a sequence of events from launch to acquisition of the Earth by the spacecraft is shown in Fig. 2.

Cruise phase. Injection (second *Agena* cutoff) occurred at 17:20:01 GMT over the western coast of South Africa at a geocentric latitude and longitude of −12.89 and 15.07 deg, respectively. The *Agena*–spacecraft combination was at an altitude of 192 km and traveling at an inertial speed of 10.949 km/sec. At 1 min, 32 sec after injection, the *Agena*–spacecraft combination entered the Earth's shadow. The *Agena* separated from the spacecraft 2 min, 35 sec after injection, performed a programmed 180-deg yaw maneuver, and ignited its retrorocket. The retrorocket impulse was designed to eliminate interference with the spacecraft operation and reduce the chance of the *Agena* impacting the Moon. Tracking data indicated that the *Agena* passed the upper trailing edge of the Moon at an altitude of 4170 km about 3 hr after *Ranger 7* impact.

Ranger 7 left the Earth's shadow 40 min, 5 sec after injection after a total shadow duration of 38 min, 33 sec. Sun acquisition had been initiated 9 min, 58 sec prior to leaving the Earth's shadow and was accomplished 5 min after leaving the Earth's shadow. Within 1 hr after

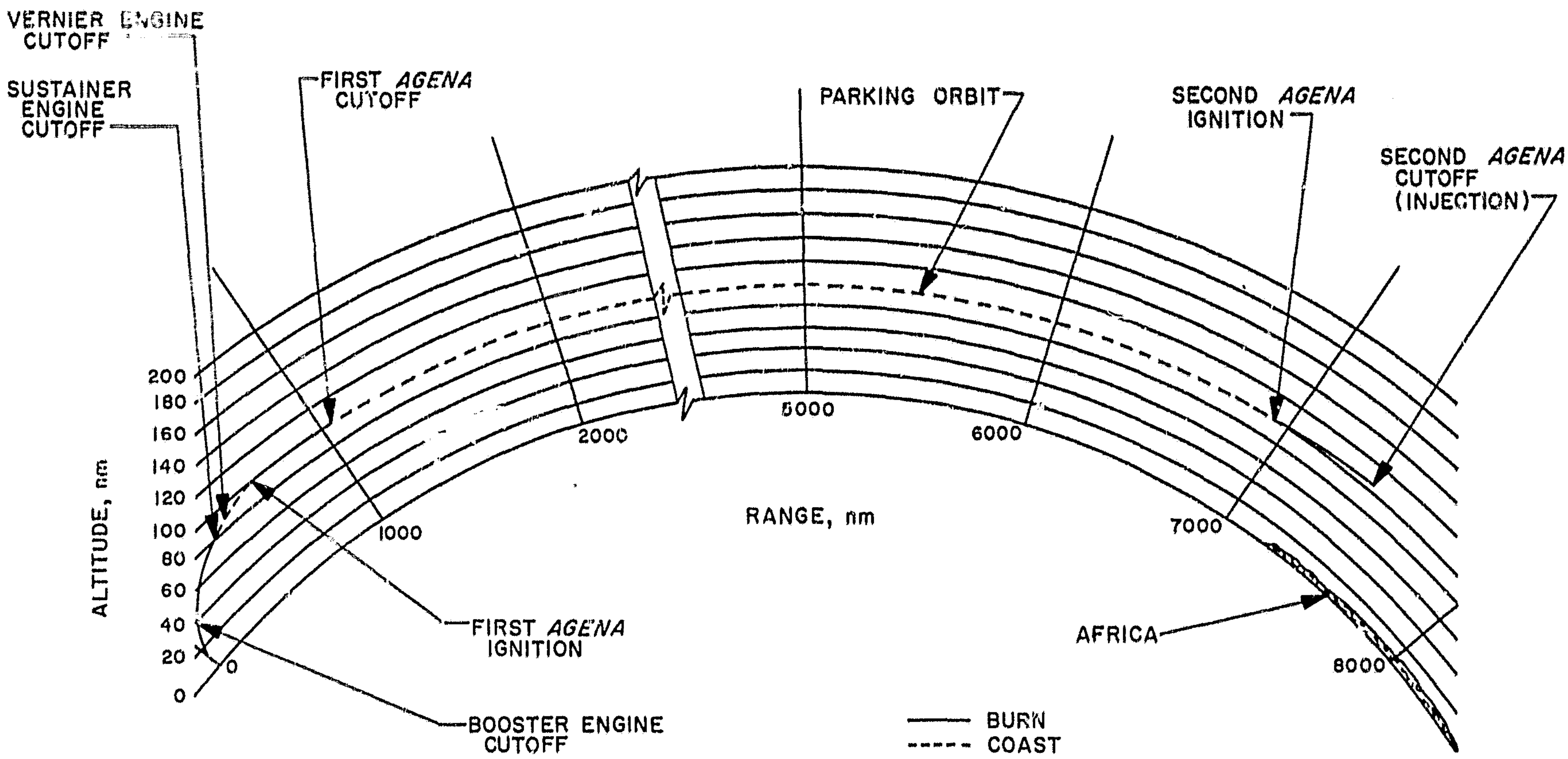

Fig. 1. Ascent trajectory profile

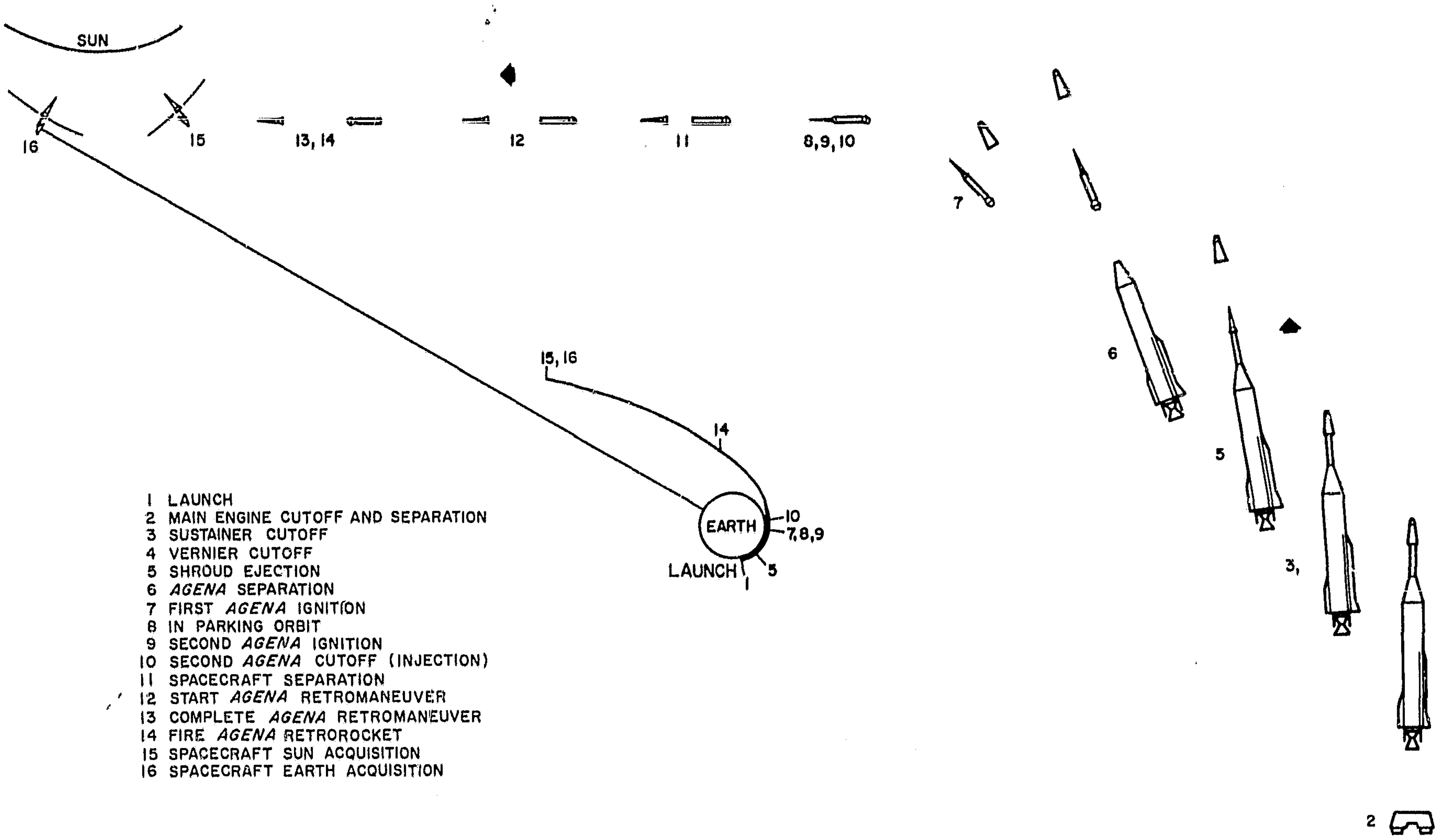

Fig. 2. Sequence of events to Earth acquisition

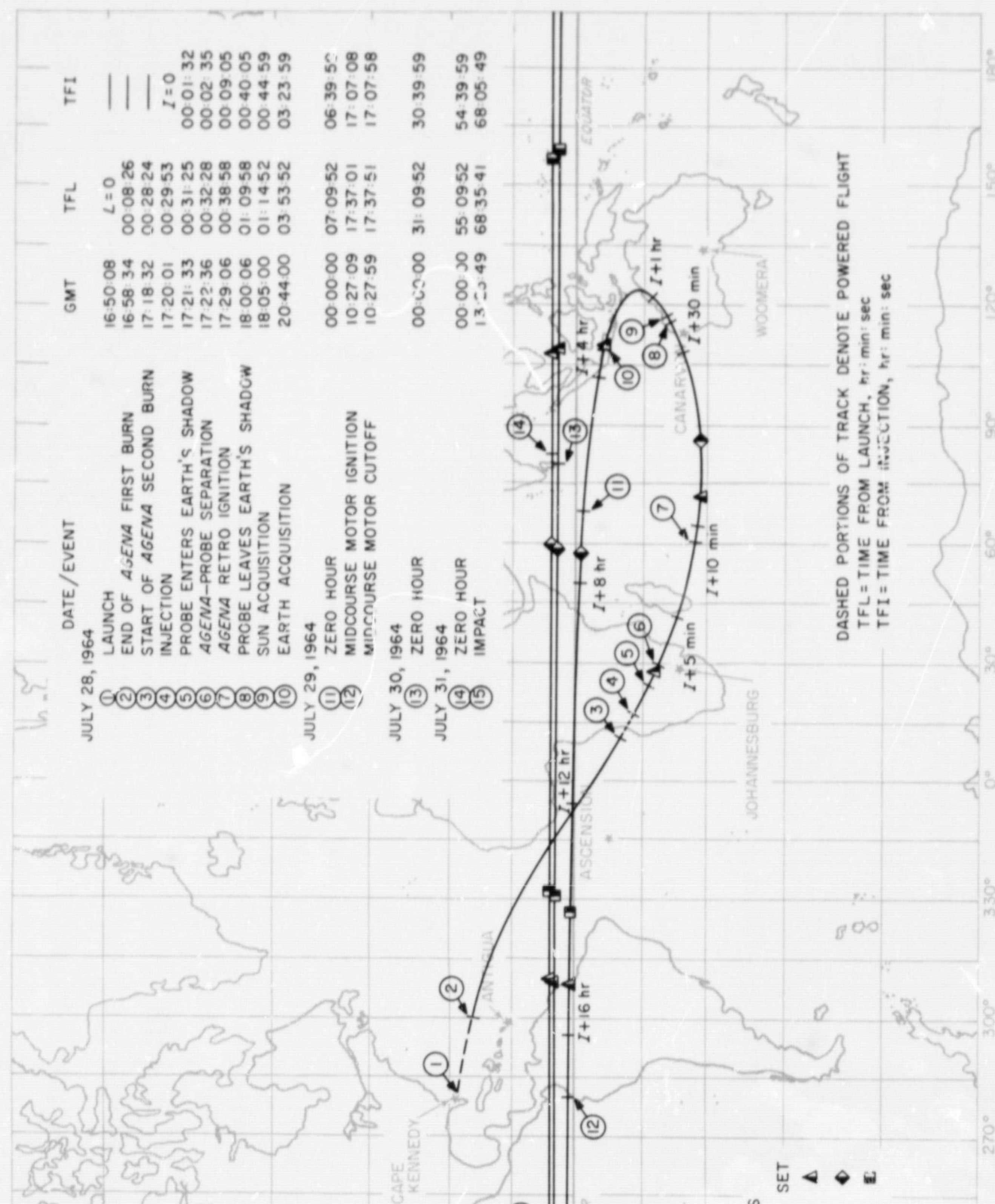

Fig. 3. Earth track of Ranger 7 trajectory

injection, the spacecraft was receding from the Earth in almost a radial direction with decreasing speed. This reduced the geocentric angular rate of the spacecraft (in inertial coordinates) until, at 1.4 hr after injection, the angular rate of the Earth's rotation exceeded that of the spacecraft. This caused the Earth's track of the spacecraft (Fig. 3) to reverse its direction from increasing to decreasing Earth longitude. Plots of the geocentric distance and inertial speed of the probe as well as the Earth-probe-Sun (EPS), Sun-probe-Moon (SPM), and Earth-probe-Moon (EPM) angles as functions of time from launch are presented in Figs. 4 through 6.

Tracking data gathered and analyzed prior to the midcourse maneuver indicated that, without a correction, the spacecraft would impact the back side of the Moon at a selenocentric latitude and longitude of −12.3 and 204.0 deg, respectively. The transit time from injection to impact would have been 67.391 hr. The *Ranger 7* transfer trajectory is illustrated in Fig. 7.

Midcourse maneuver phase. In order to alter the trajectory so as to impact a selected aiming point at a selenocentric latitude of −11 deg and longitude of −21 deg, midcourse maneuver calculations indicated a requirement

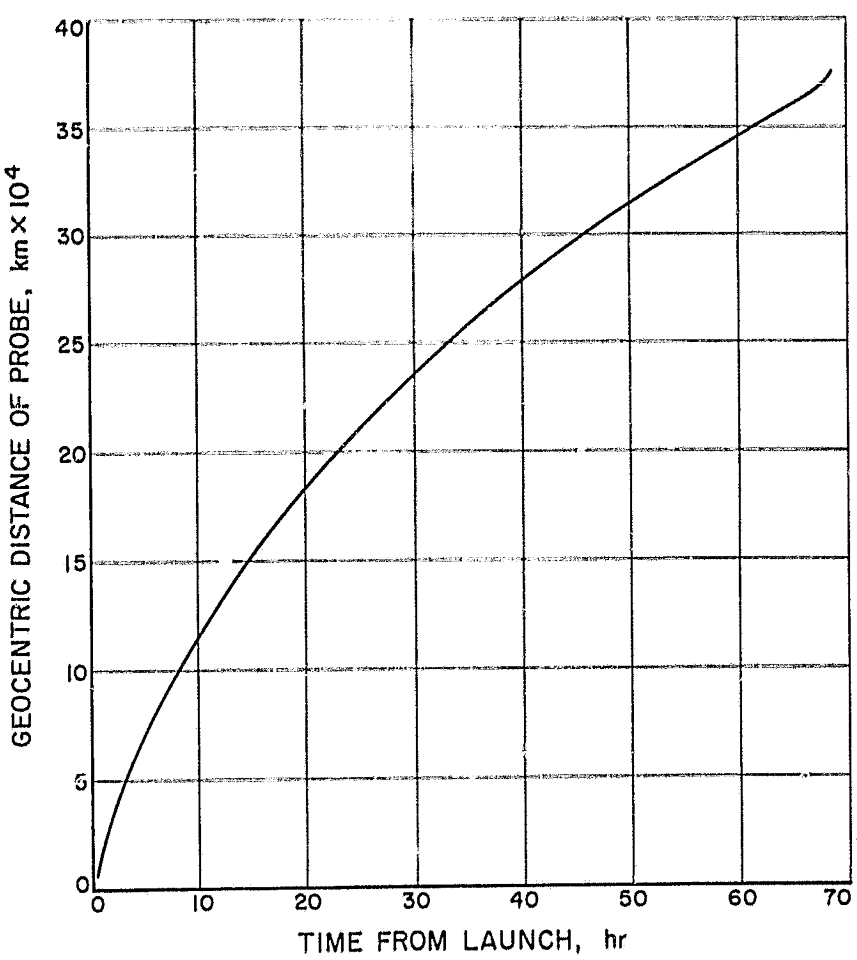

Fig. 4. Geocentric distance of probe vs time from launch

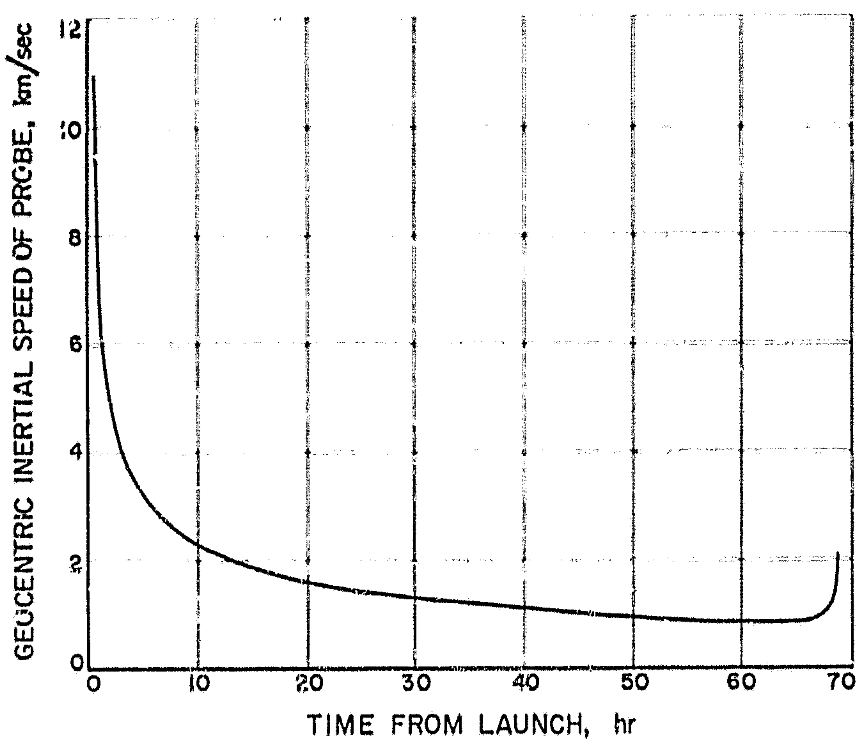

Fig. 5. Geocentric inertial speed of probe vs time from launch

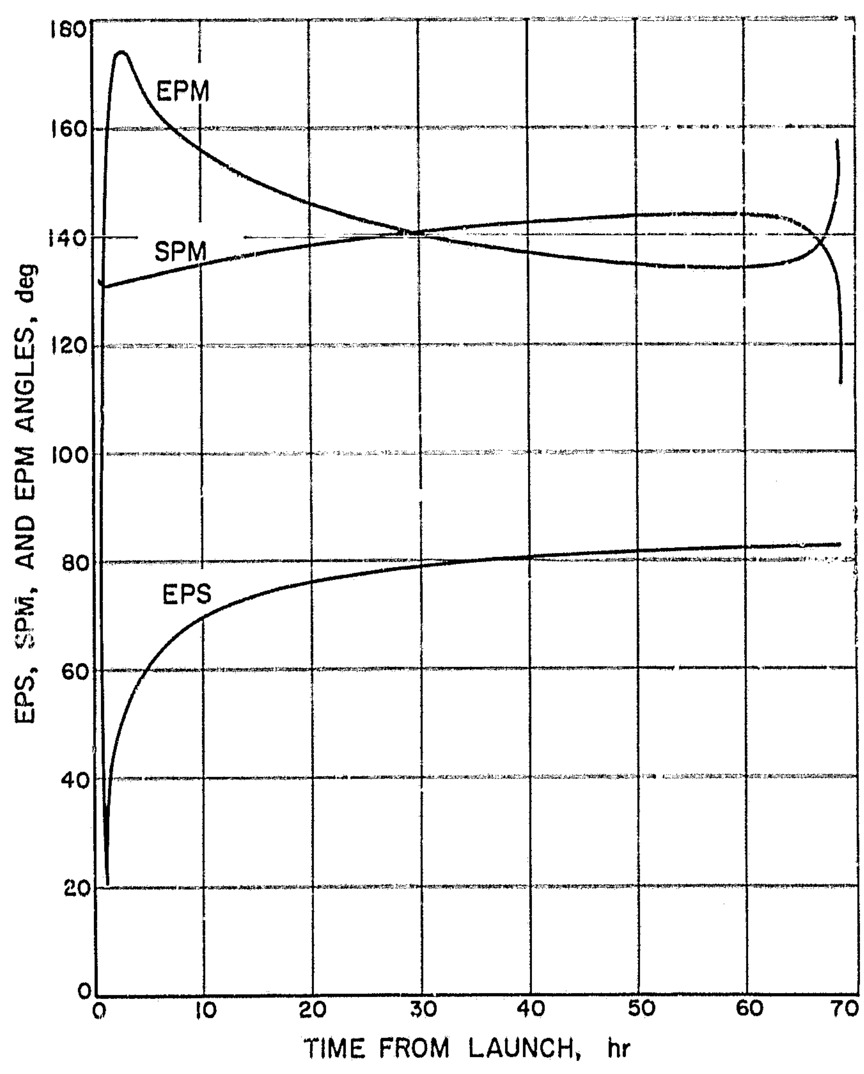

Fig. 6. Earth-probe-Sun, Sun-probe-Moon, and Earth-probe-Moon angles vs time from launch

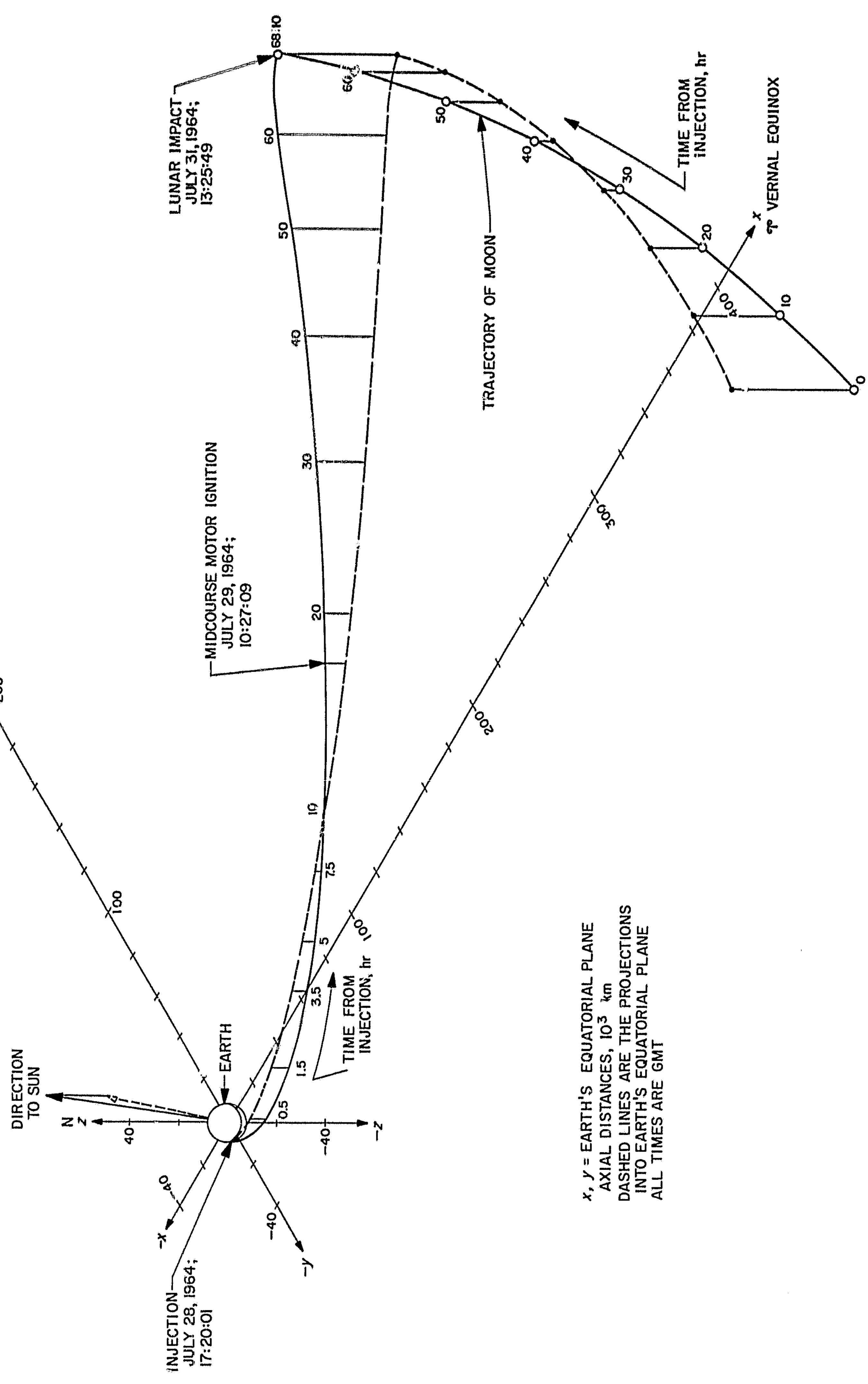

Fig. 7. *Ranger 7* **transfer trajectory**

for a 29.89-m/sec increment of velocity (60-m/sec maximum capability). In addition, this correction was selected to adjust the flight time from injection to impact to be 68.09 hr, thus allowing the TV camera backup turn-on clock to be utilized as designed. To properly align the thrust direction of the midcourse motor for the burn, a 5.56-deg roll turn and −86.80-deg pitch turn were required. The midcourse motor was ignited at 10:27:09 GMT on July 29, 1964, at which time the spacecraft was at a geocentric distance of 169,000 km and traveling with an inertial speed of 1.786 km/sec relative to the Earth. At the end of the 50-sec burn of the midcourse motor, the geocentric distance had increased to 169,075 km, and the inertial speed relative to the Earth had decreased to 1.756 km/sec. Analog data received at the Goldstone Tracking Station and relayed to the JPL Space Flight Operations Facility gave positive indication that the midcourse maneuver and motor burn had been executed precisely. This was further verified by the observed doppler data, which were essentially the same as those predicted for the maneuver. Injection and encounter conditions for the premidcourse orbit used to determine the midcourse maneuver are given in Table 1.

Postmidcourse maneuver cruise phase. Following the midcourse maneuver, the spacecraft reacquired the Sun and Earth, thus returning to the cruise mode. At about 63 hr from injection and at a geocentric distance of 355,300 km, the spacecraft's inertial speed relative to the Earth reached a minimum value of 0.850 km/sec. At this point, the spacecraft was about 28,300 km from the lunar surface with an inertial speed of 1.36 km/sec relative to the Moon. Due to the lunar gravitational field, the spacecraft's velocity then began to increase.

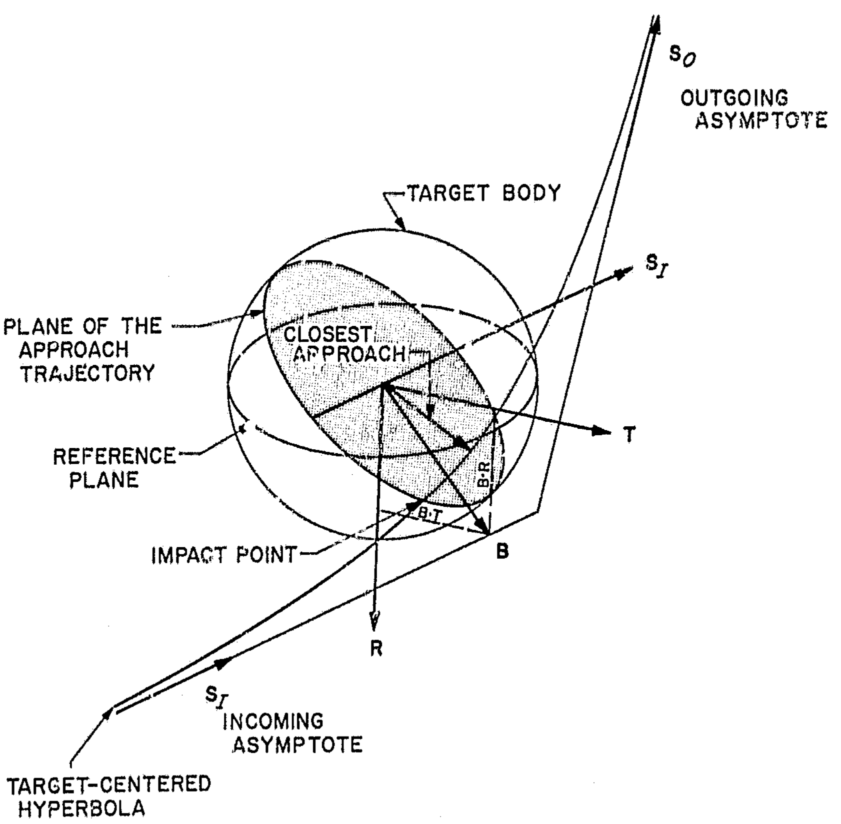

Fig. 8. Definition of the miss parameter B

Table 1. Orbit used for determination of the *Ranger 7* midcourse maneuver

Initial conditions[a]	
Epoch	July 28, 1964; 17:19:56 GMT
Earth-fixed sphericals	
R	6567.6350 km
ϕ	−12.676075 deg
θ	14.647727 deg
V	10.533237 km/sec
γ	1.3798852 deg
σ	17.37931 deg
Inertial Cartesians	
x	−4833.6829 km
y	−4206.2223 km
z	−1441.1942 km
$\dot{x}$	7.0598554 km/sec
$\dot{y}$	−6.8711888 km/sec
$\dot{z}$	−4.7802415 km/sec
Orbital elements	
a	269557.90 km
e	0.97564876
i	28.957643 deg
Ω	17.045773 deg
ω	204.26350 deg
ν	2.6878172 deg
Impact parameters	
Impact epoch	July 31, 1964; 12:43:29.17 GMT
Selenocentric latitude	−12.344962 deg
Selenocentric longitude	203.95135 deg
Time of flight from injection	67.391 hr[b]
$\lvert\mathbf{B}\rvert$	3869.9779[c] km
$\mathbf{B}\cdot\mathbf{T}$[d]	−3794.9573 km
$\mathbf{B}\cdot\mathbf{R}$[d]	758.30590 km

[a]See Table 2 for definition of symbols.
[b]1σ uncertainty of 5.2 sec.
[c]1σ uncertainty of 15.9 km.
[d]$\mathbf{B}\cdot\mathbf{T}$ and $\mathbf{B}\cdot\mathbf{R}$ are referenced to the true lunar equator (Fig. 8). (For *Ranger 7* work, the true lunar equator is used as the reference plane. If $\mathbf{N}$ is a unit vector in the lunar north direction, then $\mathbf{T} = \mathbf{S}_I \times \mathbf{N}$ and $\mathbf{R} = \mathbf{S}_I \times \mathbf{T}$.)

Postmidcourse tracking data up to within 0.5 hr before impact were analyzed and resolved the lunar encounter conditions to a high degree of accuracy. Lunar impact was indicated to occur at a selenocentric latitude and longitude of −10.68 and −20.68 deg, respectively, with a flight time from injection of 68.097 hr. The encounter

Table 2. Definition of symbols (with Earth as central body)

R	probe radius distance, km
ϕ	probe geocentric latitude, deg
θ	probe east longitude, deg
V	probe Earth-fixed velocity, km/sec
γ	path angle of probe Earth-fixed velocity vector with respect to local horizontal, deg
σ	azimuth angle of probe Earth-fixed velocity vector measured east of true north, deg
x, y, z	vernal equinox Cartesian coordinates, in km, in a geocentric equatorial system. The origin is the center of the central body. The principal direction (x) is the vernal equinox direction of date, and the principal plane (x, y) is the Earth equatorial plane of date. z is along the direction of the Earth's spin axis of date
$\dot{x}, \dot{y}, \dot{z}$	first-time derivatives of x, y, and z, respectively; i.e., Cartesian components of the probe space-fixed velocity vector, km/sec
a	semimajor axis, km
e	eccentricity
i	inclination, deg
Ω	longitude of the ascending node, deg
ω	argument of pericenter, deg
ν	true anomaly, deg

conditions and the corresponding postmidcourse initial conditions are presented in Table 3.

Encounter phase. During the encounter phase of the *Ranger 7* flight, the spacecraft raced toward destruction by lunar impact with increasing acceleration due to the pull of the lunar gravitational field. This effect is shown in Fig. 9, where the *Ranger 7* trajectory to lunar encounter is compared with a hypothetical *Ranger 7* trajectory resulting from a massless Moon. At 1 hr before impact, at a lunar altitude of 6390 km, the speed of the probe relative to the Moon had increased to 1.551 km/sec. No terminal maneuver to realign the TV cameras' pointing direction was necessary.

About 45.5 min before impact, the spacecraft crossed the lunar equator at an altitude of 4933 km. At 13:08:36 GMT, while at an altitude of 2126 km above the lunar surface, Channel-F full power was verified. At 13:12:09 GMT, at an altitude of 1723 km, Channel-P full power was also verified. At 13:25:49 GMT on July 31, 1964, *Ranger 7* crashed onto what was to be named the lunar

Table 3. Last postmidcourse orbit of *Ranger 7*

Postmidcourse conditions[a]	
Epoch	July 29, 1964; 10:27:58 GMT
Earth-fixed sphericals	
R	169075.11 km
ϕ	2.7386728 deg
θ	277.82452 deg
V	12.070902 km/sec
γ	8.1207532 deg
σ	270.95860 deg
Inertial Cartesians	
x	156674.78 km
y	63040.835 km
z	8078.5225 km
$\dot{x}$	1.4342630 km/sec
$\dot{y}$	0.97256602 km/sec
$\dot{z}$	0.28116494 km/sec
Orbital elements	
a	244087.41 km
e	0.97401678
i	28.706807 deg
Ω	16.907167 deg
ω	203.78348 deg
ν	161.92545 deg
Impact parameters	
Impact epoch	July 31, 1964; 13:25:48.50 GMT
Selenocentric latitude	−10.671182 deg
Selenocentric longitude	−20.68303 deg
Time of flight from injection	68.0965 hr[b]
$\|\mathbf{B}\|$	1811.2719 km[c]
$\mathbf{B} \cdot \mathbf{T}$[d]	1623.8932 km
$\mathbf{B} \cdot \mathbf{R}$[d]	802.29478 km

[a] See Table 2 for definition of symbols.
[b] 1σ uncertainty of 1.0 sec.
[c] 1σ uncertainty of 14.7 km.
[d] $\mathbf{B} \cdot \mathbf{T}$ and $\mathbf{B} \cdot \mathbf{R}$ are referenced to the true lunar equator (Fig. 8). (For *Ranger 7* work, the true lunar equator is used as the reference plane. If $\mathbf{N}$ is a unit vector in the lunar north direction, then $\mathbf{T} = \mathbf{S}_I \times \mathbf{N}$ and $\mathbf{R} = \mathbf{S}_I \times \mathbf{T}$.)

"Mare Cognitum" at an impact speed of 2.616 km/sec and at a path angle of −64.1 deg. The spacecraft had encountered the Moon in a direct motion along a hyperbolic trajectory, the incoming asymptote direction being at an angle of −5.57 deg to the lunar equator and with the orbit plane inclined 26.84 deg to the lunar equator.

The trace of the trajectory on the lunar surface from injection to impact is given in Fig. 10; the traces of the lunar approach portions of the premidcourse and postmidcourse orbits are illustrated in Fig. 11. Figs. 12 through 16 present trajectory parameters plotted versus GMT prior to impact of the *Ranger 7* spacecraft on the Moon.

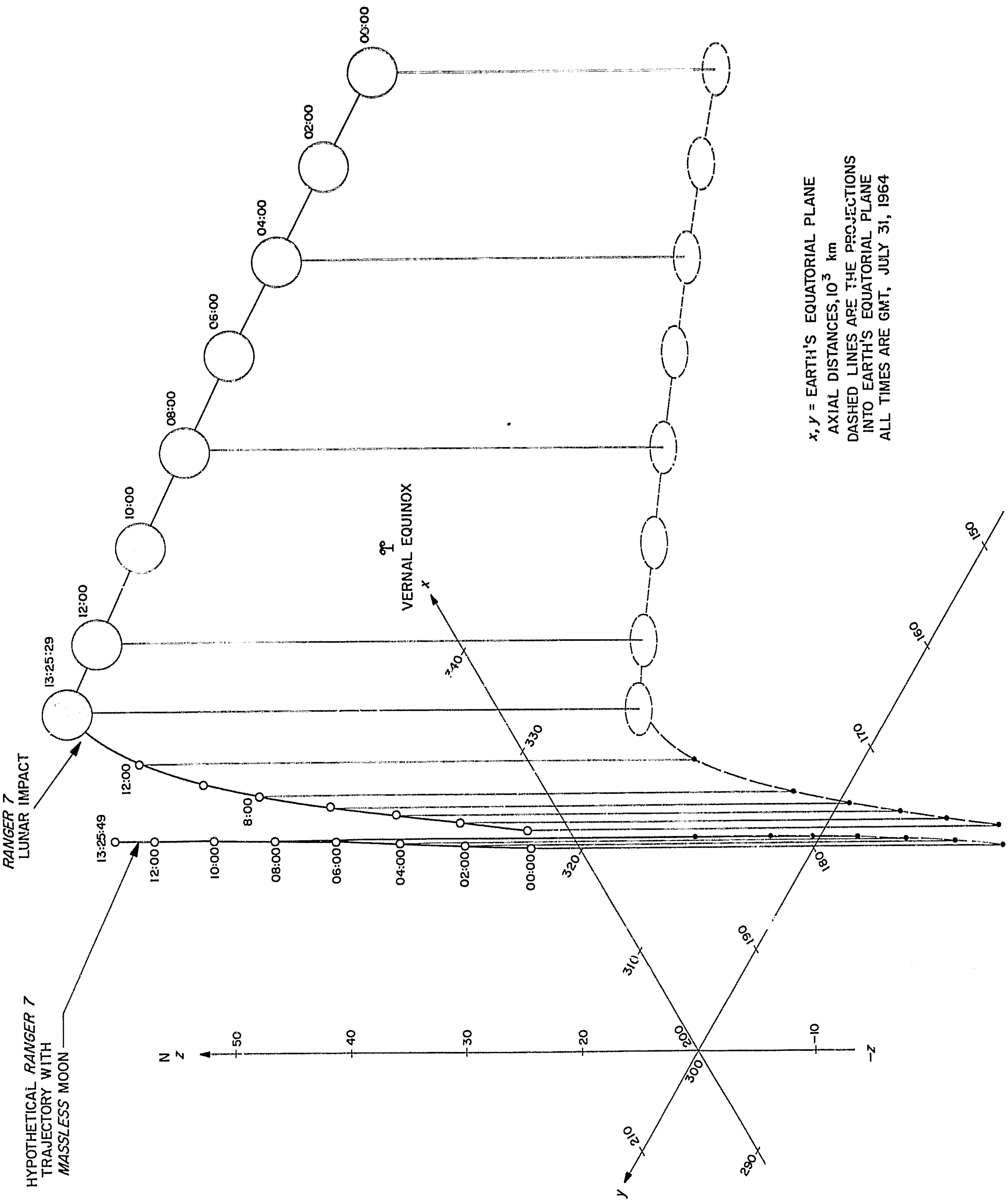

Fig. 9. Effect on *Ranger 7* trajectory due to lunar gravitational attraction

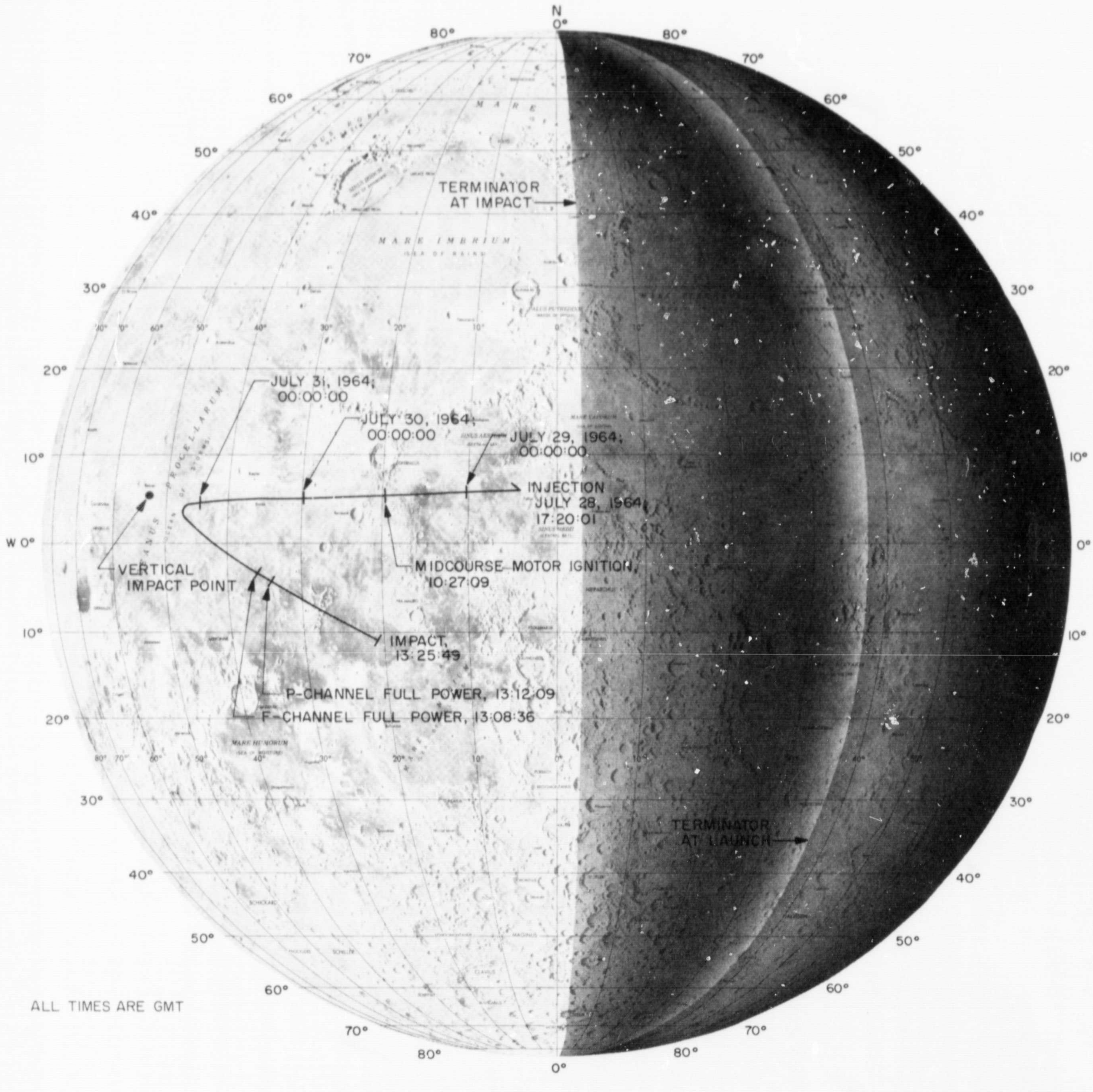

Fig. 10. Lunar track of *Ranger 7* trajectory

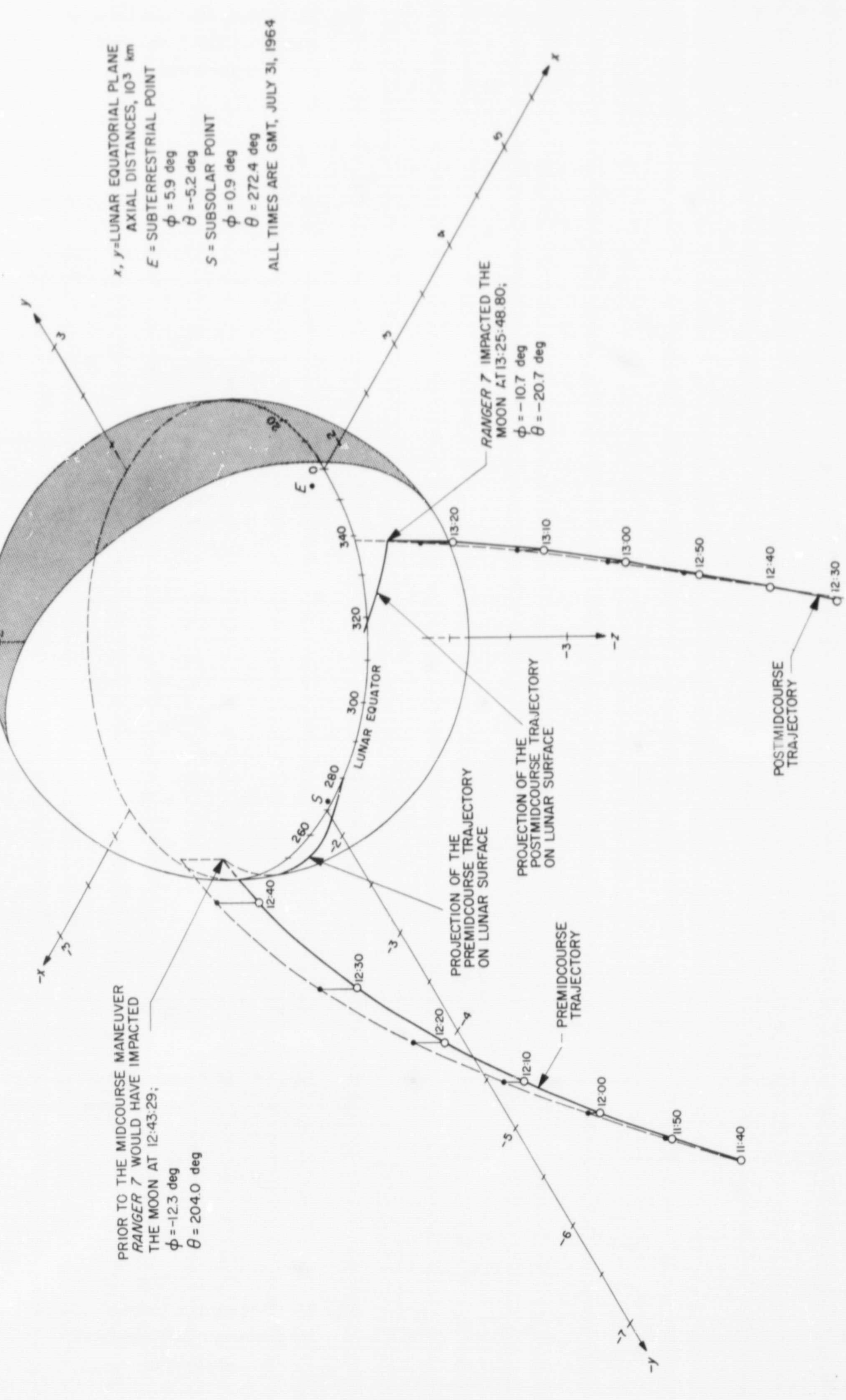

Fig. 11. *Ranger 7* **premidcourse and postmidcourse encounter trajectories**

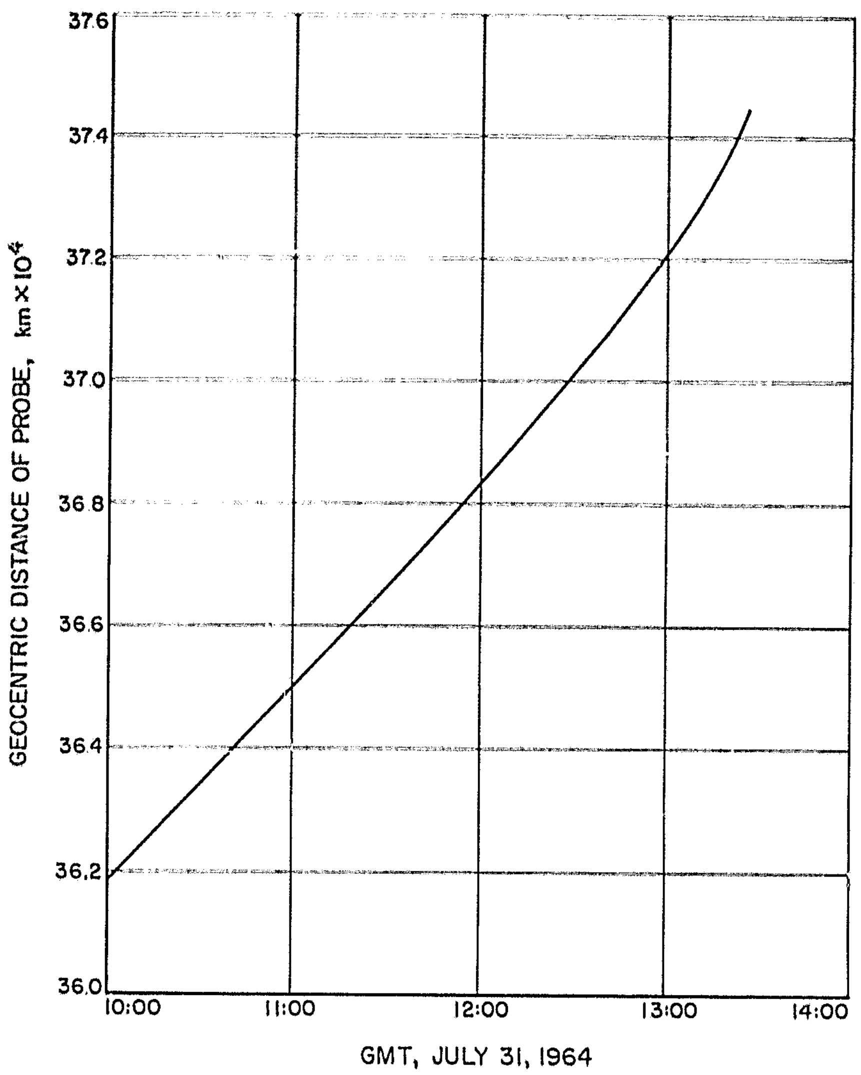

Fig. 12. Geocentric distance of probe vs GMT at lunar encounter

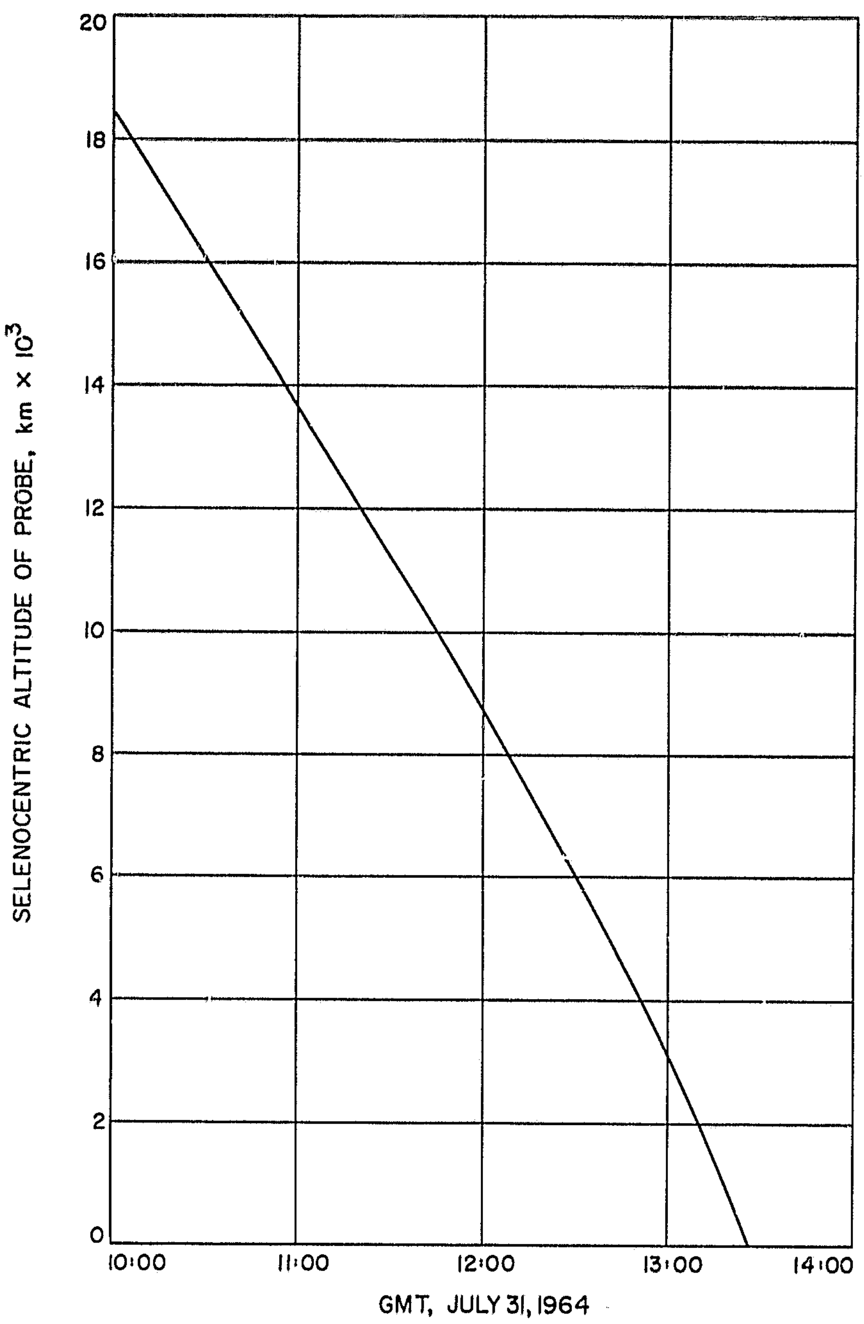

Fig. 14. Selenocentric altitude of probe vs GMT at lunar encounter

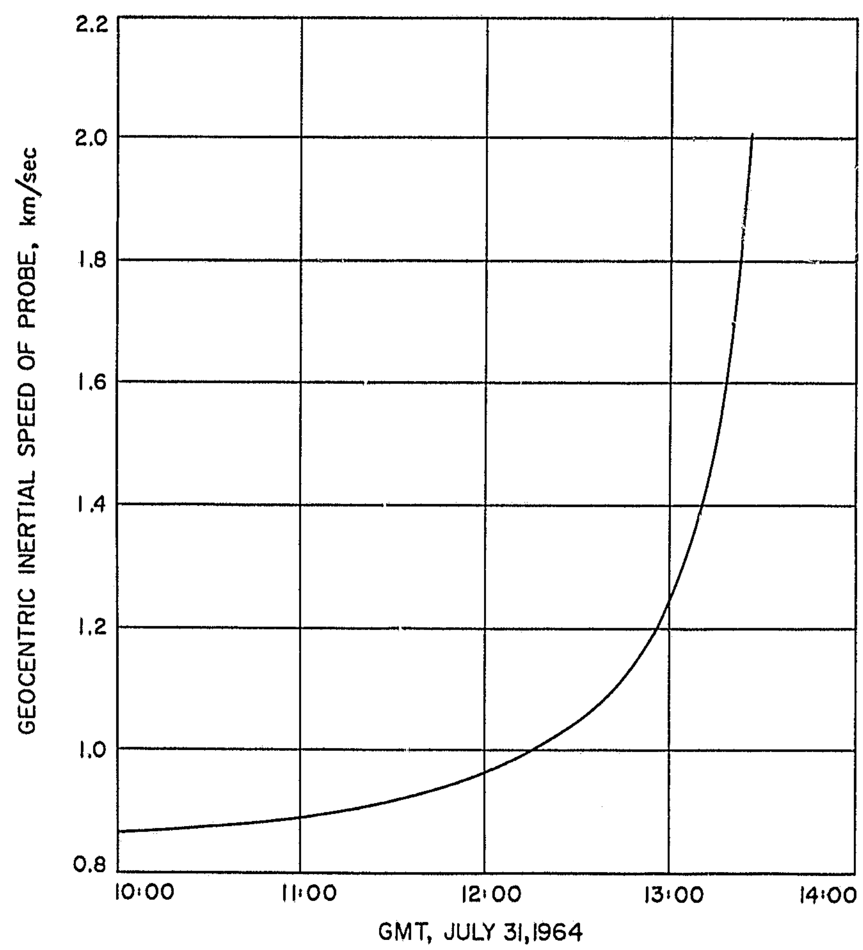

Fig. 13. Geocentric inertial speed of probe vs GMT at lunar encounter

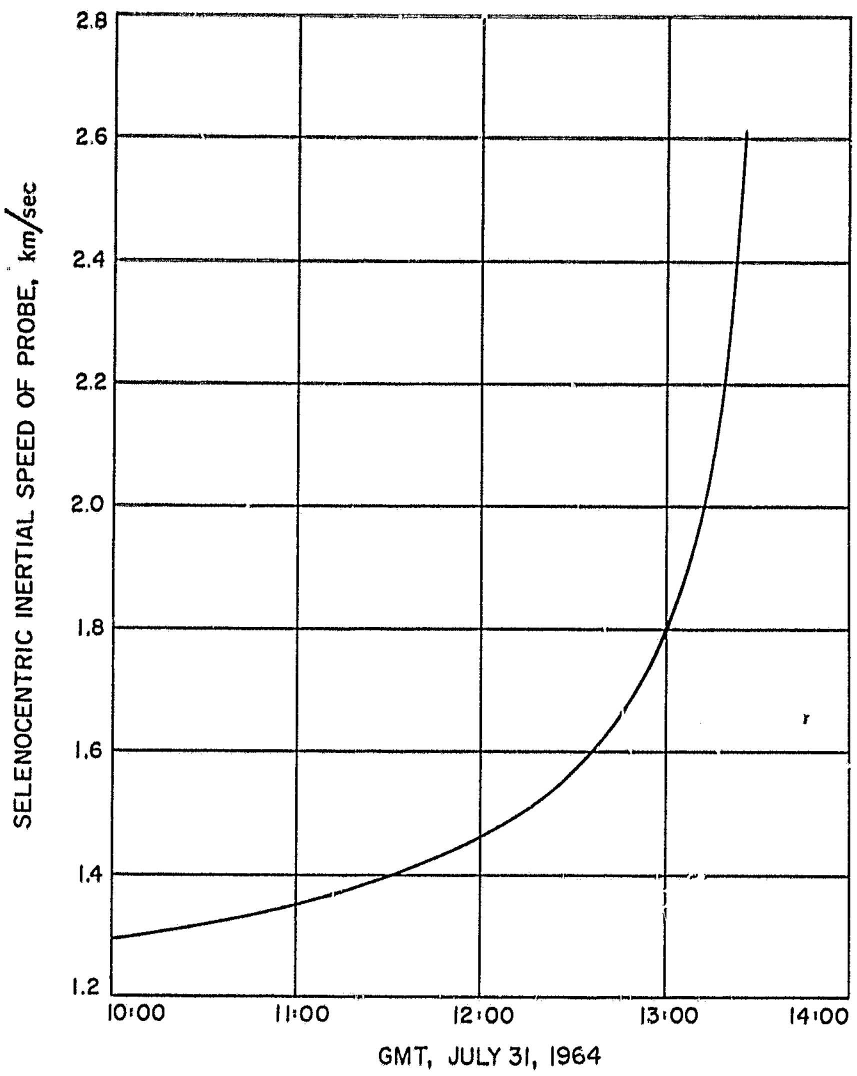

Fig. 15. Selenocentric inertial speed of probe vs GMT at lunar encounter

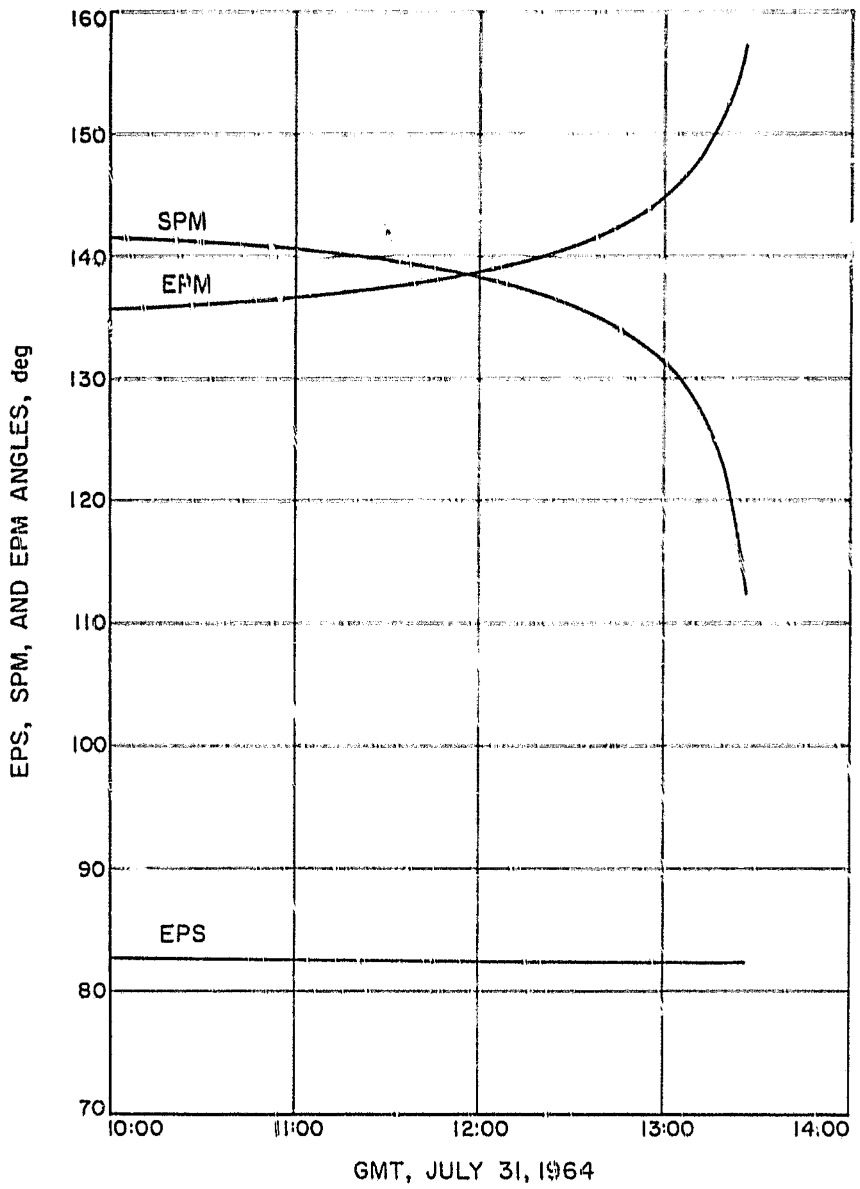

Fig. 16. Earth-probe-Sun, Sun-probe-Moon, and Earth-probe-Moon angles vs GMT at lunar encounter

II. *Surveyor* Project

A. Introduction

The *Surveyor* Project will take the next step in developing lunar technology by attempting soft landings on the Moon with a group of test missions whose objective is to demonstrate successful soft landings by post-landing spacecraft operation. An engineering payload including elements of redundancy, increased diagnostic telemetry, touchdown instrumentation, and survey TV will be used.

Following the test missions, the general objective is to conduct lunar exploration to extend our knowledge of the nature of the Moon and to discover and verify the suitability of sites for *Apollo* spacecraft landings. These flights will carry a scientific payload selected from the following experiments: two-camera TV, micrometeorite ejecta, single-axis seismometer, alpha-particle scattering, soil properties (surface sampler), and touchdown dynamics.

Through 1966 spacecraft will be injected into the lunar trajectory by direct ascent, using single-burn *Atlas–Centaur* vehicles. For launches prior to 1966, a 50-m/sec midcourse correction capability will exist. Launches performed in 1966 will require a 30-m/sec midcourse correction capability.

Hughes Aircraft Company is under contract to develop and manufacture the first seven spacecraft.

B. Spacecraft Systems Development

The following material relating to the *Surveyor* spacecraft system was prepared by the Hughes Aircraft Company. The principal model designations and vehicles discussed are defined in Table 1.

System engineering. The transponder for the SD-2 dynamic test spacecraft was tested at Goldstone and accepted by JPL in mid-September. A main power switch is being added to the spacecraft as a safety provision to enable cutoff of all spacecraft power up to launch. A preliminary telemetry calibration and error analysis handbook is being coordinated with the users. In tests at Lewis Research Center, spacecraft hardware showed no ill effects from gas impingement during operation of the *Centaur* shroud ejection system.

Scientific payload. Design was completed on a change to the alpha scattering experiment to provide for five additional data signals; an engineering change proposal for an improved instrument is being prepared. A change proposal has been completed on incorporating current limiting in the power circuits for the alpha scattering, micrometeorite ejecta detection, and seismological experiments. Vibration tests were performed on the soil

Table 1. Model and vehicle designations

Designation	Description
SC-1–4	Flight spacecraft with engineering payload
SC-5–7	Flight spacecraft with scientific payload
A-21	Model designation for spacecraft with engineering payload (SC-1–4)
A-21A	Model designation for spacecraft with scientific payload (SC-5–7)
T-21	Model A-21 prototype system test spacecraft
T-21A	Model A-21A prototype system test spacecraft
T-2	Simplified spacecraft for evaluation of terminal descent propulsion and flight control
S-2	Test spaceframe for vibration, shock, and static structural tests
S-6, -7	Test spaceframe for vernier propulsion system tests
S-8	Test spacecraft for flight control buzz tests

mechanics/surface sampler. Type approval testing of the television camera is approaching completion. Photometric charts for TV camera calibration on the Moon have been designed. A preliminary thermal analysis of the television cameras has been performed.

System analysis. Studies were made to show the effects of midcourse velocity distribution on vernier propellant requirement and the effects of increasing retro-engine separation time on terminal descent parameters. Landing accuracy was evaluated in a Monte Carlo simulation program. The use of a coherent-type threshold leading edge detector in the television system for horizontal synchronization was analyzed. A sequence analysis for the soil mechanics/surface sampler was made, and methods of reducing operating time were studied. A command verification and transmission computer program is being developed for integration into the JPL Space Flight Operations Facility.

Flight control. The flight control electronics unit completed type approval testing successfully. Further evaluation of a delayed square-wave power source for the gyro and Canopus sensor motors indicated an efficiency increase with three-phase power. Work was initiated to incorporate the slit-type acquisition Sun sensor on the first flight spacecraft. The first set of flight-type gas jet valves passed acceptance tests.

Electronics. Excessive phase jitter in the receiver and transmitter is being eliminated through ribbon mounting of the crystals. The circuitry for the RF transfer switch drive was modified to remove potential failure modes. Improvements were incorporated in the boost regulator and the battery charge regulator.

Electrical power supply. The solar panel wiring harness was redesigned for compatibility with the new mast harness and the first three flight panels were reworked to incorporate the changes. Solar cells were space-calibrated in JPL balloon flights for use as primary standard cells. Infrared radiometry is being evaluated for use in solar panel testing. Five prototype main batteries passed type approval vibration and shock tests; four have successfully passed the 300-hr type approval thermal-vacuum test.

Thermal control. An upgraded analysis indicates that the A-21 compartment system has a positive heat dissipation capability at lunar noon and a night heat loss of 20 w, compared to 60 w previously estimated. The paint pattern on the helium tank has been changed to prevent overheating in the transit phase. Special test hardware for solar-thermal-vacuum testing of the T-21 spacecraft has been defined, and a data monitoring system has been checked out. A comprehensive thermal test program employing a new spacecraft thermal control model has been started.

Engineering mechanics. Shock absorber tube failures were traced to excessive chuck pressure during machining, and corrective steps were taken. Revision of the mathematical model used in the forced-response computer program to accommodate upgrading of the S-2 vehicle to the S-2A configuration is continuing. Type approval vibration testing of S-2A was carried out, except for certain low-frequency tests that will be conducted with a redesigned motor housing in the antenna/solar panel positioner housing; the housing failed in a lateral shake test at 9.6 cps. Structural analysis and redesign were performed on the equipment compartments and the retro-engine supports.

Propulsion. The first four quality assurance firings of the main retro-rocket engine were made at Arnold Engineering Development Center; ballistic performance was satisfactory, and preliminary data indicate that thrust vector excursion met specifications. An inert engine with a modified hinge joint was vibration tested. In the vernier propulsion system program, two expulsion unbalance tests with the S-6 vehicle using simulated propellant were completed. The 30-day storage test with the S-7 vehicle, involving firings at 5-day intervals, was started. Type approval testing of the 6 Al–4 Va titanium propellant tanks is complete, except for the vibration phase.

Spacecraft vehicle and mechanisms for basic bus. Vehicle assembly operations included assembly of SC-1 for the beginning of system tests and upgrade of T-21; T-21A, SC-2, T-1, and T-2SS are in process of assembly at the close of the period. Strengthened mechanisms for deployment of the omnidirectional antennas have performed satisfactorily in vibration testing of the S-2A vehicle. A redesigned motor housing is being fabricated to replace the one that failed in S-2A vibration. Type approval testing of pyrotechnic squibs is nearly complete.

Reliability, quality assurance, and system test. In the reliability assurance test program, Canopus sensors incorporating a structural improvement have performed satisfactorily in vibration and thermal-vacuum tests; two sensors have survived 1500 hr of mission simulation and the tests are continuing. The upgraded T-21 system test spacecraft is receiving functional tests prior to the start of thermal-vacuum tests about November 1; the test equipment has been checked out with generally satisfactory results. Preparations are being made for the T-21 vibration and shock tests. The T-2S descent test vehicle completed closed-loop tests simulating the first drop test scheduled for October 20. A vibration test of the S-8 vehicle with the radar altimeter and doppler velocity sensor installed, using simulated vernier engine vibration inputs, is being planned. The S-8 buzz test suspension system was checked out. The System Test Equipment Assembly (STEA) 3 system is being prepared for testing the SC-2 spacecraft.

Mission operations. Planning details for the *Surveyor/Centaur* combined system test are being coordinated. The three operations consoles for use at the Air Force Eastern Test Range (AFETR) have undergone tests, and one has been modified for use with the *Surveyor* dynamic models. Compatibility testing of the dynamic model transponder for SD-2 in conjunction with Deep Space Instrumentation Facility equipment was completed at the Goldstone Pioneer Site. Microwave installation and testing was conducted at AFETR.

Support of study on critical data recorder. Hughes provided technical support to the Aeronutronics Division of Philco in their study of a critical data recorder (CDR) for installation on the *Surveyor* spacecraft. The purpose of the CDR is to sense and transmit data on spacecraft structural condition and orientation even after a landing hard enough to make the spacecraft inoperative. The Hughes effort included coordination and preliminary design on CDR mounting, data channel assignments, mechanical loads, thermal and radiation environments, a breakwire sensing system, and test and operations requirements.

PLANETARY–INTERPLANETARY PROGRAM

III. *Mariner* Project

A. Introduction

The early objective of the Planetary–Interplanetary Program is the initial probing of the planets Mars and Venus by unmanned spacecraft. The initial probing of Venus was successfully accomplished by *Mariner 2*. The next step toward this objective is the initial probing of Mars by a *Mariner C* spacecraft planned for the 1964–1965 opportunity.

The primary objective of the *Mariner C* missions (*Mariner* Mars 1964 Project) is to conduct closeup (flyby) scientific observations of the planet Mars during the 1964–1965 opportunity and to transmit the results of these observations back to Earth. The planetary observations should, to the greatest practical extent, provide maximum information about Mars. TV and cosmic dust experiments, as well as a reasonable complement of field- and particle-measurement experiments, will be carried on the *Mariner C* spacecraft. In addition, an Earth occultation experiment will be carried on spacecraft launched during the Type I trajectory launch period to obtain data relating to the scale height and pressure in the Mars atmosphere. The Project Office has the option of launching one spacecraft on a Type II trajectory and waiving the occultation experiment on this mission if, in its judgment, such action maximizes the probability of success of the total mission.

A secondary objective is to provide experience and knowledge concerning the performance of the basic engineering equipment of an attitude-stabilized flyby spacecraft during a long-duration flight in space farther away from the Sun than the Earth. An additional objective is to perform certain field and/or particle measurements in interplanetary space during the trip and in the vicinity of Mars.

The *Atlas D–Agena D* launch vehicle to be used in this Project has a capability of injecting a separated spacecraft weight of 570 lb (minimum) into a mass transfer orbit.

It is planned to conduct two launchings of *Mariner C* spacecraft from two separate launch pads. All activities will be planned to exploit the limited launch period to the maximum extent. To accomplish this, spacecraft and launch vehicles will be processed in parallel so that, following the launch of the first spacecraft (*Mariner C-2*), the second (*Mariner C-3*) may be launched without delay, no earlier than 2 days after the first.

Planned testing of *Mariner C-2* at the Air Force Eastern Test Range (AFETR) was completed, and the final joint flight-acceptance composite test (J-FACT) and simulated launch were conducted successfully and on schedule. Following completion of system tests at JPL in mid-September 1964, *Mariner C-3* was shipped to the AFETR, where it has undergone complete retesting. At the end of October, *Mariner C-3* was moved to the launch complex, where it was mated to the *Atlas D–Agena D* launch vehicle for the J-FACT scheduled to follow the *Mariner C-2* launch. On September 29, the *Mariner C-4* spacecraft arrived at the AFETR, where it has undergone system verification testing. *Mariner C-4* is being maintained as an assembled set of tested spares for backup of the flight spacecraft. Each flight solar panel has been degaussed, reducing its magnetic field (which varied from 5 to 26 gamma) to approximately 0.4 gamma.

On October 7, a formal prelaunch Project review meeting was held at the AFETR with representatives from NASA Headquarters. The status of each system was reviewed in detail. At that time, no problem areas in any of the systems were known which would have precluded launching on schedule.

B. Spacecraft Systems Testing

1. First Flight Spacecraft, Mariner C-2

After completing all scheduled tests at JPL, *Mariner C-2* was shipped to the AFETR on August 23, 1964. A system verification test and the initial AFETR system test were performed. The spacecraft then underwent mechanical preparation for movement to the launch complex.

The *Atlas* was erected on the launch pad on September 14. During this operation, a stretch sling failed. Although the launch vehicles were not damaged, the booster flight-acceptance composite test was delayed 2 days as a precautionary measure to allow further investigation.

The *Mariner C-2* electrical tests were completed successfully, the flight shroud was installed, and the RF checks were satisfactory. The spacecraft was moved to the launch pad on September 18 and mated with the *Agena*. Power and functional tests began the following day; difficulties encountered in the blockhouse with data encoder and science functions were later corrected.

The first part of the simulated countdown was completed on September 21 after approximately 8 hr of testing. Problems with the data encoder did not delay the operations. The second part of the countdown was completed on September 23, and it was concluded that the simulated countdown would have resulted in launch in a real situation.

A successful J-FACT was run on September 25. Because of problems which occurred during the first part of the simulated countdown, this part was repeated on September 27 with only one anomaly: the umbilical lanyard did not retract. This problem was later resolved.

After the shroud and adapter were removed, weight and center-of-gravity measurements were made. The weight was found to be 575 lb. The spacecraft was then partially disassembled and moved to the explosive safe area for an attitude-control leak test. Magnetic mapping showed gamma values which varied somewhat from those obtained during the last JPL survey, but the deviation was not considered critical. Following mapping operations, *Mariner C-2* science calibrations were again verified.

The final system test was completed October 13 after 86.2 hr of testing. A cruise-science statistical-data quiet test was then performed. Following final electrical reverification on October 14, all spacecraft systems were pronounced "go" in a post-test critique, and the spacecraft was released for final mechanical flight preparations.

The spacecraft was moved to the explosive safe area on October 21. During mating operations with the *Agena* adapter, a problem developed with the shroud umbilical door. The problem was resolved following an investigation by the Lockheed Missiles and Space Company.

Final mechanical flight preparations were completed on October 26, and the spacecraft was moved to the launch pad and mated with the *Agena* the following day. The spacecraft on-pad functional test was completed without problems. A power transient caused a minor problem during the on-pad simulated countdown; otherwise, all operations were normal.

A near-perfect J-FACT was performed October 31; the only delay was a 40-min hold for a launch on a nearby pad. Only minor variations from the actual launch countdown procedure were permitted. As of November 1, the *Mariner C-2* spacecraft was ready for launch.

2. Second Flight Spacecraft, Mariner C-3

Mariner C-3 System Test 3 was performed July 23 to 25, 1964, at JPL with satisfactory results, except for uneven motion of the scan platform, difficulty with the narrow-angle Mars gate, and a faulty TV target. Values of 30 to 40 gamma were obtained during the magnetic mapping operations which followed.

Many problems were encountered during the vibration tests, particularly while the flight solar panels were being installed. During the vibration on both spacecraft axes on August 5, only minor difficulties occurred.

A verification test was followed by weight and center-of-gravity determinations in full flight configuration (except for the postinjection propulsion system motor). A free-mode test performed August 8 was satisfactory, except for certain noncritical anomalies in the radio subsystem.

Several problems were encountered during the system verification test that preceded the JPL Space Simulator operations: some of the coaxial cables failed; an Earth ground connection was damaged; a power operational support equipment (OSE) connector was faulty; and trouble developed in the TV subsystem. After these problems were corrected, the vacuum chamber was pumped down and a test was conducted August 13 to 24. Principal problem areas were the attitude-control vacuum system, the solar vanes, the plasma high-voltage power, and the cosmic ray telescope. Operation of the scan platform appeared smooth.

Following an acceptable system test and preparations for shipment, the *Mariner C-3* spacecraft was shipped to the AFETR on September 7. Visual inspection after its arrival revealed no damage to the spacecraft resulting from shipment. After calibration of the spacecraft TV head end assembly and electronics, a system test was started September 18. Canopus acquisition required more time than usual. The Sun gate lamp failed, and difficulties were encountered in the TV OSE control panel. The ion chamber was removed for incorporation of a JPL engineering change requirement. The system test was completed September 22. Electrical tests of the spacecraft, with and without shroud, were also completed that day, and the spacecraft was then prepared for matchmate operations. These operations were completed September 28, requiring less time than those for *Mariner C-2*.

The explosive-safe-area electrical tests and an attitude-control leak test were then performed. On October 7, the spacecraft science equipment was removed for laboratory calibration. A second matchmate test with the *Agena* adapter was conducted October 8. The *Mariner C-3* spacecraft was then moved to the launch complex and mated with the *Agena*.

3. Backup Spacecraft, Mariner C-4

The *Mariner C-4* spacecraft, assembled from flight spares, will be maintained as a field backup for *Mariners C-2* and *-3*. On July 22, 1964, mechanical buildup of the spacecraft at JPL had progressed to a point where the first electrical tests could be performed, including power, data encoder, pyrotechnics, attitude-control, flight command, and central computer and sequencer subsystem checks. The mechanical assembly continued concurrently and was completed August 11.

Intersubsystem (except for radio Cases V and VI) tests were performed July 28 to 30. The attitude-control gas system was installed and, on July 31, most of the science equipment was on the spacecraft. Science interface and subsystem tests followed.

The spacecraft was then prepared for system testing. System Test 1 was conducted August 12 to 14. Problems were experienced with power amplifier and radio exciter switching, a defective connection in the scan platform, and varying receiver–local oscillator drive. Other minor problems occurred, but the over-all system test was considered successful.

The start of *Mariner C-4* vibration testing was delayed to allow incorporation of all equipment. The first verification test was run August 20 without problems. A special magnetometer test was performed to determine the cause of magnetometer interference from the TV subsystem during *Mariner C-2* system testing. The results indicated that, when the magnetometer transformer–rectifier is powered by a separate supply, the interference is removed.

The first lateral-axis vibration was performed August 22, and the second lateral-axis vibration and the z-axis shake followed the next day. A failure occurred in the pyrotechnics arming switch, and a spare was installed. Weight and center-of-gravity determinations were made, and a system test was run August 26 to 28 without major problems. A system verification test and a JPL Space Simulator test followed. During the Simulator test, the facility lost vacuum while the spacecraft was operating in a critical mode. This caused oil to spray over the spacecraft, affecting the ion chamber, radio, central computer and sequencer, and cosmic dust detector. *Mariner C-4* was then disassembled, and the hardware was inspected and retested. By September 9, the spacecraft was reassembled, and a verification test was performed on September 11 with only minor anomalies. The Space Simulator test was completed September 15 with no major problems.

After being disassembled and subjected to a satisfactory thermal test, *Mariner C-4* was shipped to the AFETR on September 25. Reassembly of the spacecraft was completed by October 2. A system verification test revealed only minor OSE problems, and a system test was satisfactorily completed October 6.

The spacecraft was then disassembled for final inspection. (*Mariner C-4*, unlike *Mariners C-2* and *-3*, did not undergo final inspection at JPL.) A detailed system verification test followed. The spacecraft is being held in a "standby" condition, except for isolated special tests.

C. Spacecraft Thermal Testing

The *Mariner C* flight spacecraft were subjected to thermal tests in the JPL 25-ft Space Simulator to verify that the thermal design is adequate and to predict flight temperatures. On the basis of the data obtained, it can be concluded that the thermal-control design is not sensitive to the unavoidable variations in tolerances between spacecrafts. An inconsistency in the temperature of the ion chambers was traced to variation in the properties of the ion chamber sphere. Other spacecraft-to-spacecraft variations are unexplained but within tolerance.

These tests also yielded an estimate of the effects of operational-support-equipment cabling on spacecraft temperatures. Comparison of temperatures obtained during a minimum-cable test (thermal test) and those obtained in a normal system test indicated that cabling lowers bus temperatures. The system test produced bus temperatures 2 or 3°F lower than those obtained during the thermal test. This was probably due to heat leakages caused by the system test equipment and cables. Flight temperatures are expected to be 1 or 2°F higher than the temperatures indicated during the thermal test. This result applies only to the *Mariner C* cabling configuration; different routing and thermal treatment of operational-support-equipment cables would produce different results.

D. Design and Development

1. Video Storage Subsystem

By the fall of 1962, *Mariner C* mission requirements had been sufficiently defined to indicate a definite need for spacecraft onboard data storage of approximately 5×10^6-bits capacity. At that time, the development of a recorder having a capacity of 10^6 bits had been completed, using one data track on a 300-ft endless loop and capable of synchronous playback at 8.33 bits/sec. In addition, a 10^7-bit recorder was under development, using three data tracks and one sync track on a 700-ft endless loop and capable of synchronous playback at low tape speeds. A 10^8-bit reel-to-reel recorder was also being developed.

Because of the stringent reliability requirements imposed on the spacecraft design by the 9-month *Mariner* mission and the short time available for subsystem design and fabrication, it was decided to utilize a recorder system similar to those already developed. After considering the data-storage requirements imposed by a *Mariner*-type mission and the relative progress of the 10^6-, 10^7-, and 10^8-bit recorder development programs, functional specifications were defined for the *Mariner C* recorder system as follows:

The video storage subsystem (recorder system) records digitized TV data during a planetary encounter or flyby and reproduces these data at a much lower rate following the encounter. The recorder system accepts fully serial, return-to-zero data from the data automation system at a fixed rate of 1.07×10^4 bits/sec and stores a minimum of 5.24×10^6 bits of video data, equivalent to 20 TV

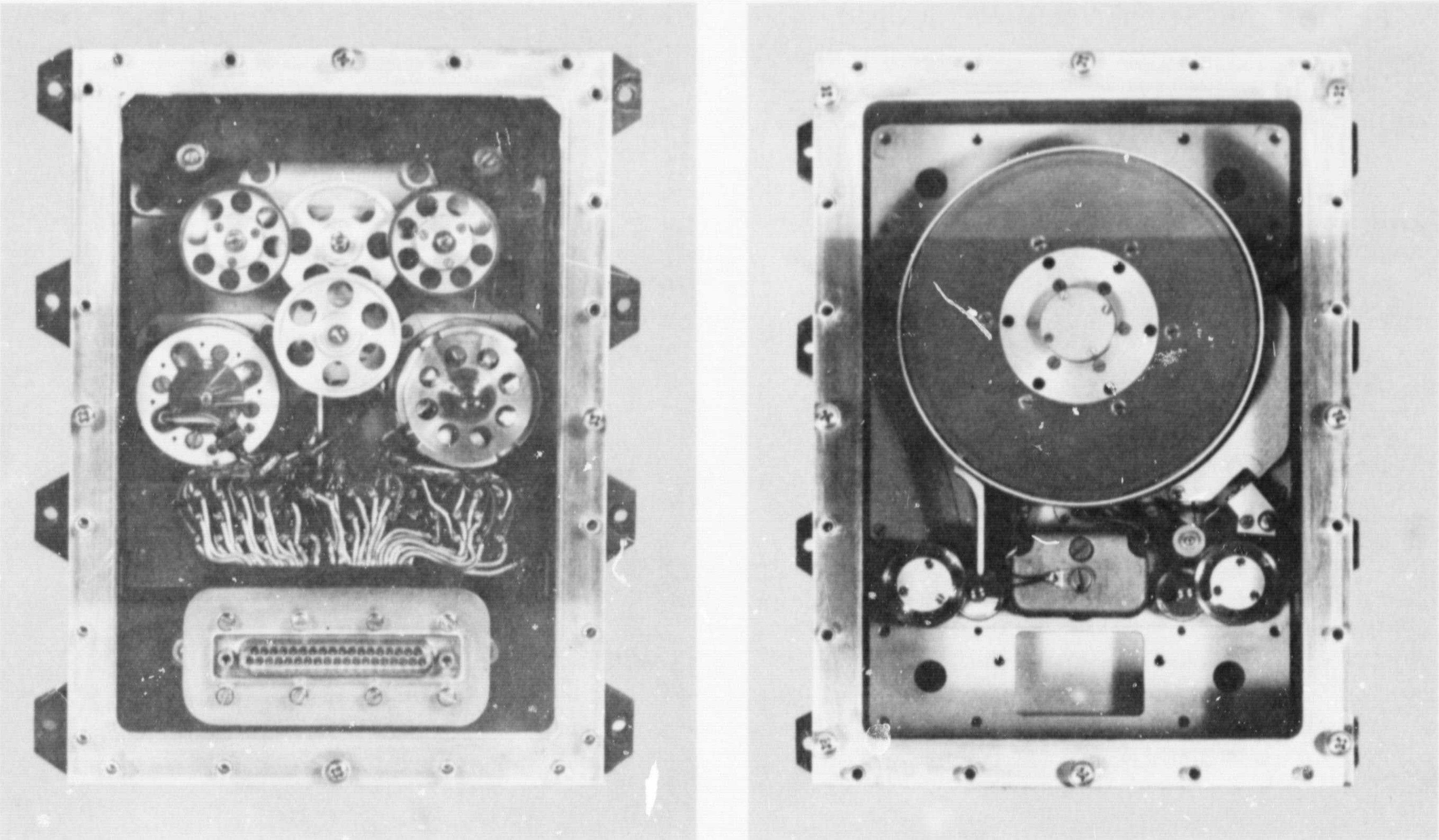

Fig. 1. Tape transport subassembly, showing drive motors, heads, and playback preamplifiers

pictures, using two data tracks on a 330-ft loop. It reproduces, for coding by the data encoder, synchronous, fully serial, nonreturn-to-zero, binary data at a fixed output rate of 8.33 bits/sec. Provisions are included for operating the recorder system, in a limited sense, during launch. This mode of operation terminates shortly after separation of the spacecraft from the *Agena*.

The video storage subsystem is packaged in four standard JPL electronic subchassis in a hermetically sealed unit. (The hermetic seal maintains a sufficiently high pressure inside the case to prevent evaporation of critical recorder lubricants.) The tape transport subassembly is shown in Fig. 1.

The prototype design and fabrication phase of the video storage subsystem development was completed in February 1964. The functional and detailed design was complete at that time and has since remained essentially unchanged.

BLANK PAGE

DEEP SPACE NETWORK

IV. Deep Space Instrumentation Facility

A. Introduction

The Deep Space Instrumentation Facility (DSIF) utilizes large antennas, low-noise phase-lock receiving systems, and high-power transmitters located at stations positioned approximately 120 deg around the Earth to track, command, and receive data from deep space probes. The DSIF stations are:

Station	Location
Goldstone Pioneer	Goldstone, California
Goldstone Echo	Goldstone, California
Goldstone Venus (R&D)	Goldstone, California
Goldstone Mars (AAS; under construction)	Goldstone, California
Woomera	Island Lagoon, Australia
Canberra (under construction)	Canberra, Australia
Johannesburg	Johannesburg, South Africa
Madrid (under construction)	Madrid, Spain
Spacecraft Monitoring	Cape Kennedy, Florida

To improve the data rate and distance capability, a 210-ft antenna is under construction at the Goldstone Mars Station, and two additional antennas of this size are planned for installation at overseas stations. Overseas stations are generally operated by personnel of the respective countries.

B. Tracking Stations Engineering and Operations

1. Flight Project Engineering

a. Mariner C Project

Pioneer Station. The original S-band system, installed in the S-band Annex Building, underwent a series of tests in September and October 1964, including a command procedures test, two ground communications tests, two facility integration tests, and an operational readiness test. In addition, numerous individual subsystem tests were performed to verify all interfaces and parameters.

The Canberra S-band system was assembled and operationally tested in the Manned Space Flight Net Annex Building. Currently, the Madrid S-band system is being installed in the east wing of the Pioneer Control Building (Fig. 1). Subsystem testing of the digital and analog instrumentation assemblies has begun. Full operational testing is scheduled for late November, with completion and shipment to Madrid scheduled for early 1965.

Echo Station. Since the completion of the *Ranger 7* mission, the L-band system has been held in a "standby" condition. Testing of the Madrid S-band cassegrain cone assembly was performed using the Echo 85-ft antenna. The testing included antenna patterns, ellipticities, far-field measurements, and star tracks. The cone has been removed from the antenna and is undergoing final ground testing prior to its preparation for shipment to Madrid.

Venus Station. Because of its 100-kw transmitting capability, the Venus 85-ft az-el antenna may be used for command transmission during the final phases of the *Mariner C* mission. For this usage, a 100-kw cassegrain cone transmitter was constructed for operation on 2116 Mc. A series of ground tests of the two 100-kw power amplifiers was performed, with operation up to full power. The cone transmitter was also mounted on the antenna to establish the mating interfaces, with operation at full power. Current plans call for an interchange of the standard Venus 2388-Mc cone with the *Mariner C* cone transmitter, if needed for the *Mariner* mission, thus permitting the Venus Station to continue with its regularly scheduled planetary and star tracking activities. Testing with the separate *Mariner C* equipment will be performed when the transmitter exciter is installed.

The *Mariner C* 100-kw transmitter exciter (Fig. 2) was designed and fabricated at Goldstone. Commercially available units were used where possible, with locally designed and fabricated units being produced for specific usage peculiar to the over-all design. Since the only interface with the Venus S-band equipment is in the use of the high-voltage power supply and antenna drive equipments, the exciter was designed as a completely self-contained unit. Its output is coupled to the multiplier chain in the antenna-mounted cassegrain cone through a 1500-ft coaxial cable. The multiplier raises the final output frequency to 2116 Mc, with 3 to 4 w of drive power, and couples it into a directional switch. This directional switch permits the selection of either power amplifier for primary transmission, with the standby unit available for immediate use. A water load is also contained within the cone for power measurements. All signal and control cables and power and coolant lines

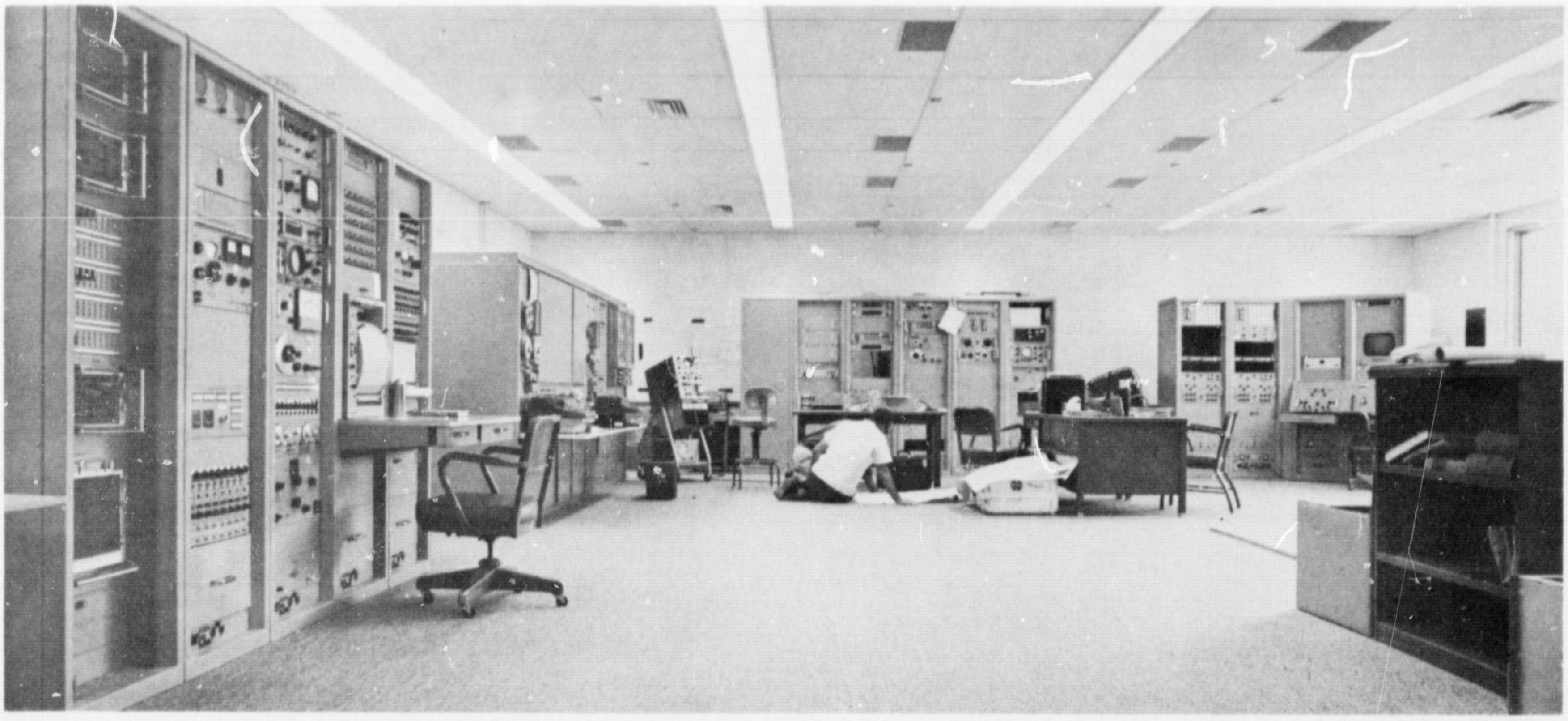

Fig. 1. Madrid S-band system installation at the Pioneer Station

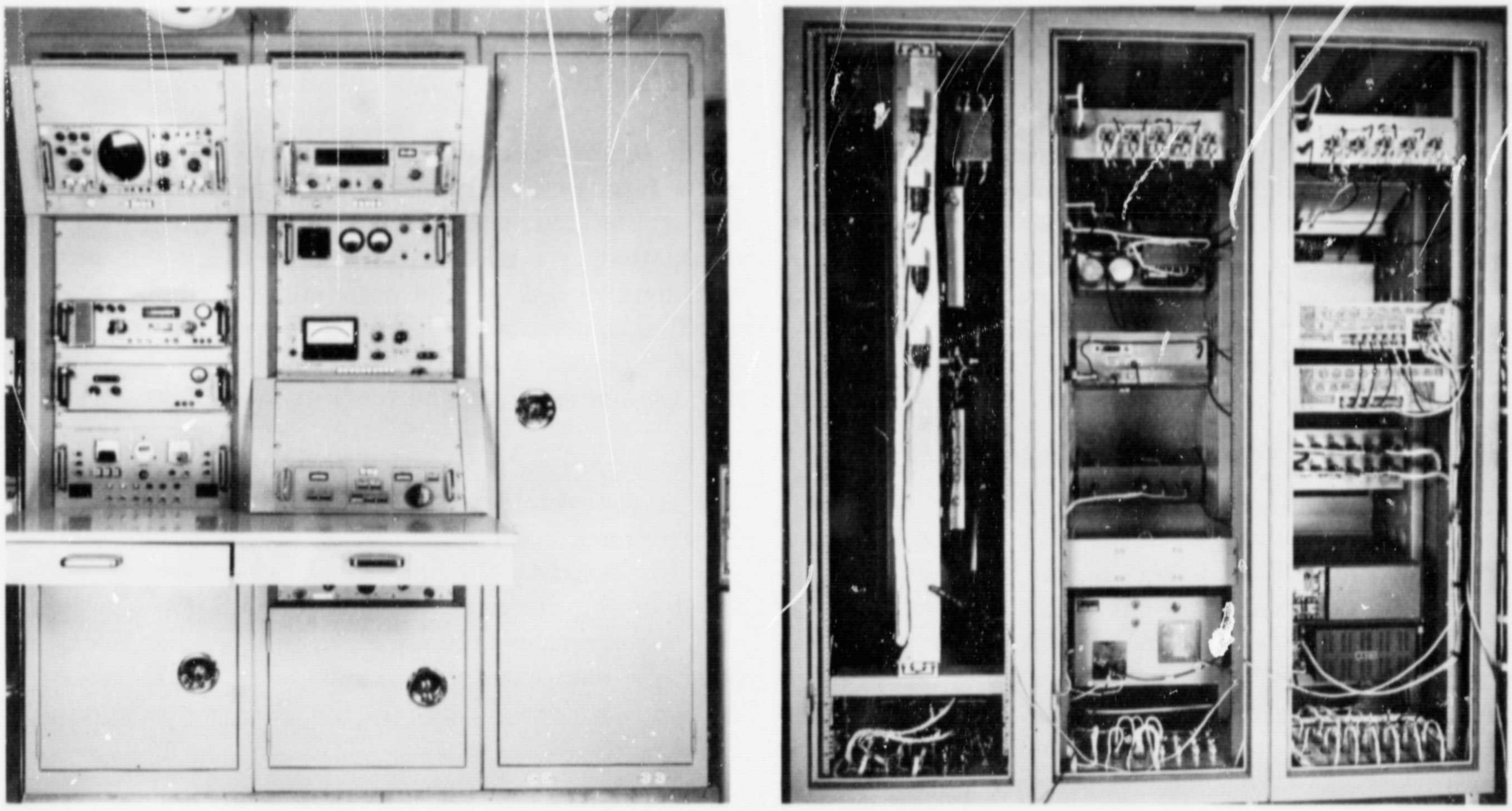

Fig. 2. *Mariner C* transmitter exciter

are brought into the cone from the bottom, through the center of the antenna. The cone can be ground-tested in the Venus Station high-voltage building and held in readiness for installation on the antenna if needed. Currently, performance tests, including installation and removal of the cone from the 85-ft antenna, are being performed.

b. Surveyor Project. Testing of the *Surveyor* ground equipment at the Pioneer Station is continuing. Investigations are in progress of the problems encountered during the DSIF/*Surveyor* compatibility tests performed during June and July. In September, a DSIF/*Surveyor* dynamic model test was performed to determine the up-link and down-link thresholds by varying the space loss between the Spacecraft Test Facility screen room and the Pioneer Station. Transmission was examined for spectral purity, and "spacecraft" telemetry was successfully received and recorded. Evaluation of the results is continuing in preparation for further testing.

2. Antenna Engineering

a. Special shipping containers. Special shipping containers were designed for the cassegrain cone and hyperbola to prevent them from experiencing shock inputs in excess of 5 *g* during the expected severe shipping and handling conditions. The containers embody shock recorders to monitor the transit conditions and are mechanized for moisture sealing. The cassegrain-cone containers are also mechanized to maintain the cone RF plumbing under dry nitrogen pressurization.

b. DSIF test trailer. A mobile instrumentation trailer was developed to facilitate all phases of DSIF antenna structural and mechanical measurements, which are an integral part of the acceptance program for new antennas being added to the Deep Space Network (DSN). The trailer will also be used to make periodic quality verification and maintenance tests on all DSN antennas to monitor their conformance to DSIF criteria and to point out areas which need attention.

The instrumentation in the trailer will accept such a variety of transducer inputs that almost any parameter of interest may be processed. Predetection recording of raw data will be made to ensure that the original data is preserved for any additional processing at JPL. In its present configuration, the trailer is capable of handling simultaneously any number of inputs up to 24, with mechanization for expansion to 48 channels on a limited basis. The instrumentation incorporates all necessary equipment to provide both "quick-look" and permanent records of all channels, and contains all calibration and general test equipment needed for field operations.

In addition to the electronic instrumentation equipment, the trailer houses a small machine shop, equipment storage, air-conditioning equipment, an electronic repair shop, desk space, film processing devices, and a 35-mm data film projector for on-the-spot analysis of boresight film camera records. The complete trailer is easily transported both locally and overseas.

3. *Telemetry-to-Teletype Data Encoder*

The telemetry-to-teletype data encoder (Fig. 3) is part of the mission-oriented operational support equipment located at each DSIF station. Its function is to encode digital data and control signals originating from either *Mariner C* or *Ranger* Block III telemetry demodulation and decommutation equipment into a format consisting of sequences of binary-coded characters suitable for teletype and/or high-speed data transmission to the Space Flight Operations Facility for subsequent information processing.

The primary output of the data encoder is a teletype paper tape which is punched with the coded-character format. The information on the punched tape is read and transmitted by a teletype transmitter–distributor unit. A secondary output of the data encoder duplicates the coded-character format in binary voltage form, which is readily converted into a form suitable for high-speed data transmission by an auxiliary unit.

The data encoder is operable in either a *Mariner* or *Ranger* configuration, but not both simultaneously. The configuration appropriate to the intended mission is switch-selected by the operator. In either configuration, the data encoder interjects real time, station identification, and spacecraft identification between the blocks of telemetry data characters as composite blocks, referred to simply as time blocks. In the *Ranger* configuration,

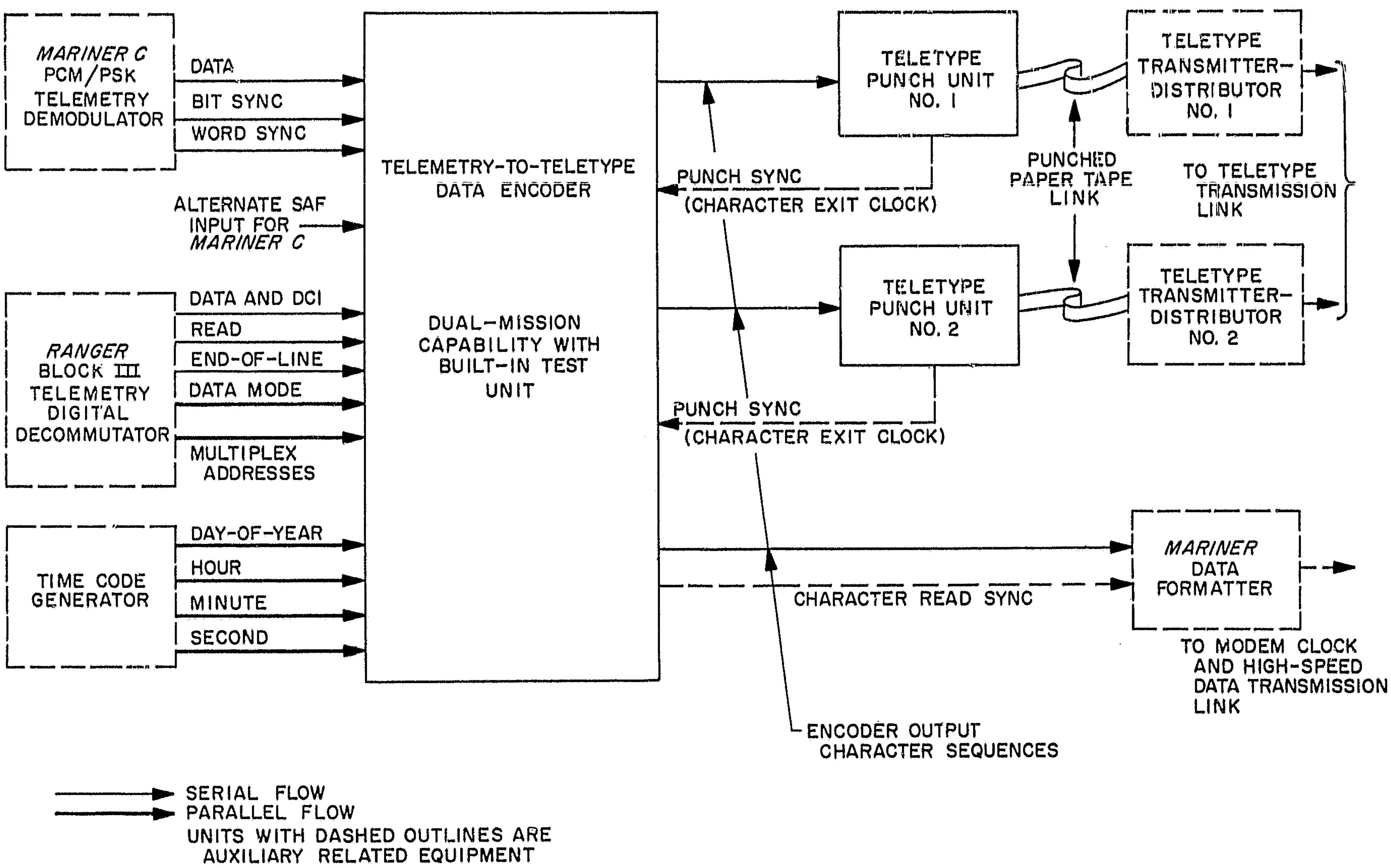

Fig. 3. Telemetry-to-teletype data encoder, *Mariner C* and *Ranger* Block III configurations

these time blocks also include decommutation address characters.

4. Telemetry Display Assembly

The telemetry display assembly (Goldstone Duplicate Standard equipment) provides a means of displaying automatic-gain-control and static-phase-error measurements locally at the station control and monitor console and remotely at the S-band receiver. During the coming *Surveyor* and *Pioneer* missions, the assembly will receive inputs from a digital instrumentation subsystem, which will remotely control the signals. If measurements other than the automatic gain control and static phase error are required, the programming of the digital instrumentation subsystem will take control and output the required information, which will be displayed at both the console and the receiver. These measurements will be provided for the *Mariner C* mission also, utilizing inputs provided by the *Mariner C* decommutator. Since data, address, and a clock signal are available, it will be possible to select at the console the desired address to be displayed by the two display panels (Fig. 4).

5. Angular Error Correction Coefficients for Use in Orbit-Determination Programs

To improve the quality of the angular tracking data going into an orbit-determination program, the data are first corrected for optical pointing errors. These are systematic errors which can be removed by applying angular error correction coefficients determined from a series (preferably more than five) of independent, horizon-to-horizon star tracks. Angular error coefficients are provided for the Woomera and Johannesburg Stations, since these are the only prime angle data stations at the present time. Although the Pioneer and Echo Stations include star tracking for subsystem tests, correction coefficients are not computed for these stations.

To ensure the validity of the coefficients used in describing the systematic errors, star tracks are conducted as a preflight calibration test and are analyzed at the Echo Station. A polynomial curve fit is made to the differences between the refraction-corrected ephemeris values and the observed values read from the angle encoders. The angular error coefficients, based on the latest optical alignment, are used in the polynomial. These coefficients

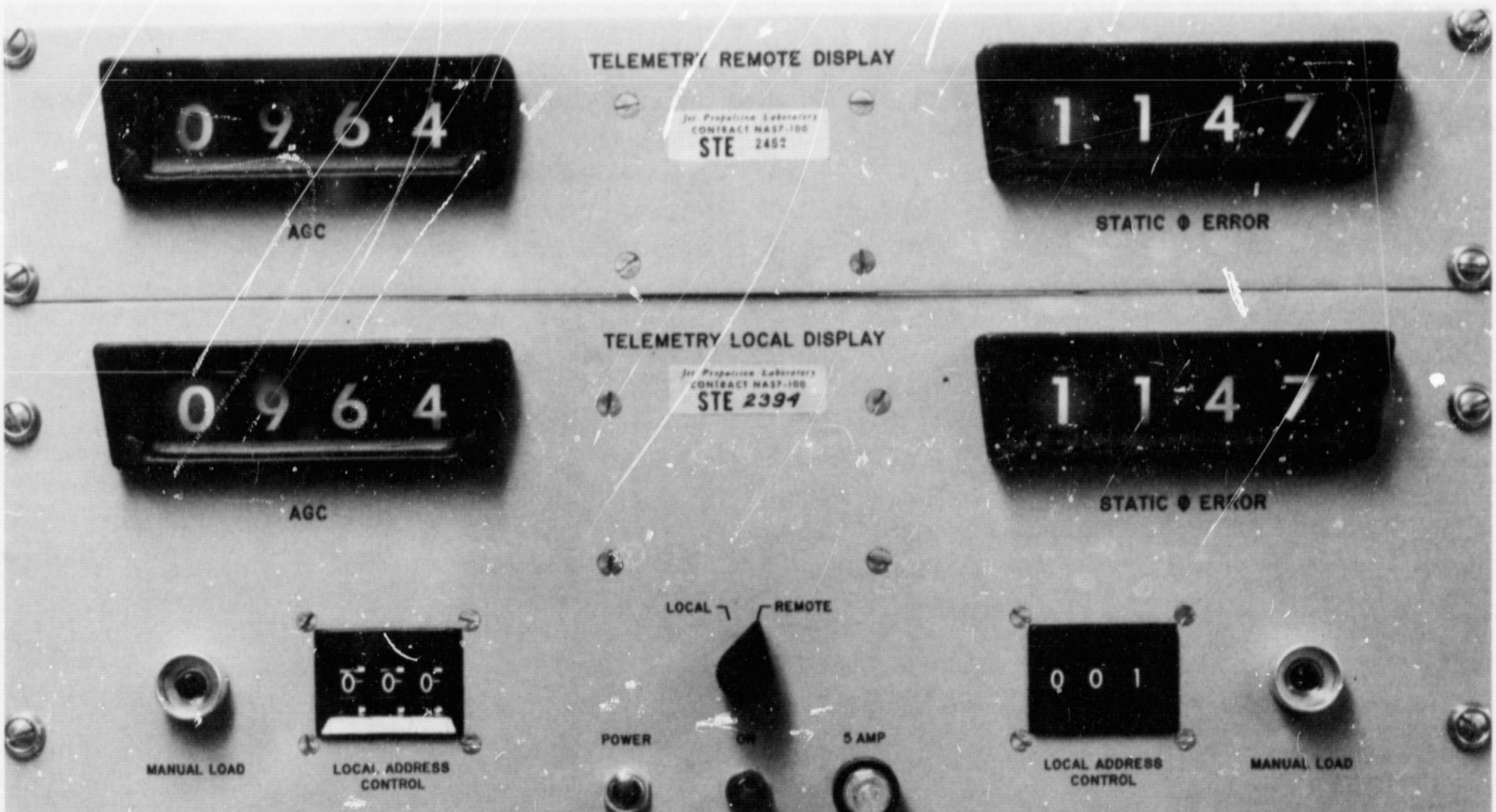

Fig. 4. Telemetry display panels

are computed with a two-dimensional curve fit program written for the IBM 7094 computer.

From the data generated, graphs are prepared with the star track reduction program and the polynomial curve fit program to determine if these coefficients will describe the optical pointing errors. It is quite probable that a new set of coefficients will be required because of a major antenna modification (L- to S-band conversion) recently completed at the stations. Graphs prepared prior to the antenna structural modification (retrofit operation) at the Johannesburg Station showed the present coefficients could reasonably describe the systematic errors.

However, later graphs, prepared after the retrofit operation and prior to the *Ranger 7* mission, showed that a new set of coefficients was needed to represent the new optical pointing errors. In addition, the inflight angular data from *Ranger 7* showed that the correction polynomials used in the orbit-determination program to describe the angular pointing error were not adequate. The old correction coefficients were used due to the heavily committed schedules at the stations and the short time period between the completion date of the antenna modifications and the *Ranger 7* launch date. New coefficients, however, were generated and tested for use in the orbit-determination program for the *Mariner C* mission.

6. Ground Instrumentation for the Mariner C Occultation Experiment

The *Mariner C* occultation experiment (to measure the perturbations produced by the refraction of the Martian atmosphere on the radio signal received at DSIF stations) places unique demands on the measurement capabilities of the DSIF. It now appears that the probability of obtaining meaningful measurements can be improved by using the second channel of the S-band receiver in a constant-frequency, constant-gain mode; the first receiver channel would be used in its normal phase-lock mode and with essentially conventional doppler and signal amplitude instrumentation. The receiver configuration described here (Fig. 5) is being considered for use in measuring the occultation phenomena.

One reference channel is operated in the normal phase-lock automatic-gain-control mode, in which telemetry, doppler frequency, and dynamic and static automatic-gain-control voltages are obtained in real time. The second reference channel is operated as a fixed-gain receiver, with a constant voltage applied to the manual gain control. The first local oscillator is derived from a frequency synthesizer locked to the station frequency standard. A relay-operated switch selects either the normal voltage-controlled oscillator or the synthesizer to drive the multiplier chain. The second local oscillator is derived from a modified 20-Mc oscillator which at present is free-running. To remove frequency instabilities and the need for recording the frequency of this oscillator, it is tied into the station frequency standard. The locked 20-Mc oscillator will perform all the functions of the present free-running unit. Narrow-band filtering is accomplished at 10 Mc to eliminate foldover.

The third local oscillator uses a 10-Mc frequency also derived from the station standard and beats the signal down to an audio frequency which is determined by the received signal frequency and the setting of the synthesizer. The present maximum predicted frequency rate of change will require a local-oscillator frequency change at approximately 5-min intervals. It is planned to have a precomputed step time–frequency function manually operated. The gross accuracy of the frequency can be validated in real time by comparison with the normal receiver voltage-controlled-oscillator frequency. After amplification, the audio frequency signal is sent to a data-processing unit. The signal is then recorded on a telemetry-type tape recorder and is digitized later.

A prime requirement of the recording is that the frequency not be distorted by more than a fraction of a cycle per second. This can be achieved in the recording band by recording a frequency standard on one track and using it as a time base for keying the digital voltmeter measuring the data channel. After digitization, a digital computer is used to detect and analyze the signal. This processing yields both frequency and power functions of time. The signal-to-noise ratio of the received signal can be obtained by comparing the power spectral density of the noise due to the system temperature with the signal power.

This basic recording technique has been successfully employed at the Venus Station for analysis of signal returns in planetary radar experiments. The only recommended modifications to the Venus radar techniques are those necessary to adapt the measurements to the operational DSIF equipment. The change from occultation mode and the normal phase-lock mode of the second receiver channel can be made in a fraction of a second by actuating three relays. (The normal configuration of the first receiver channel remains unchanged.) This is desirable

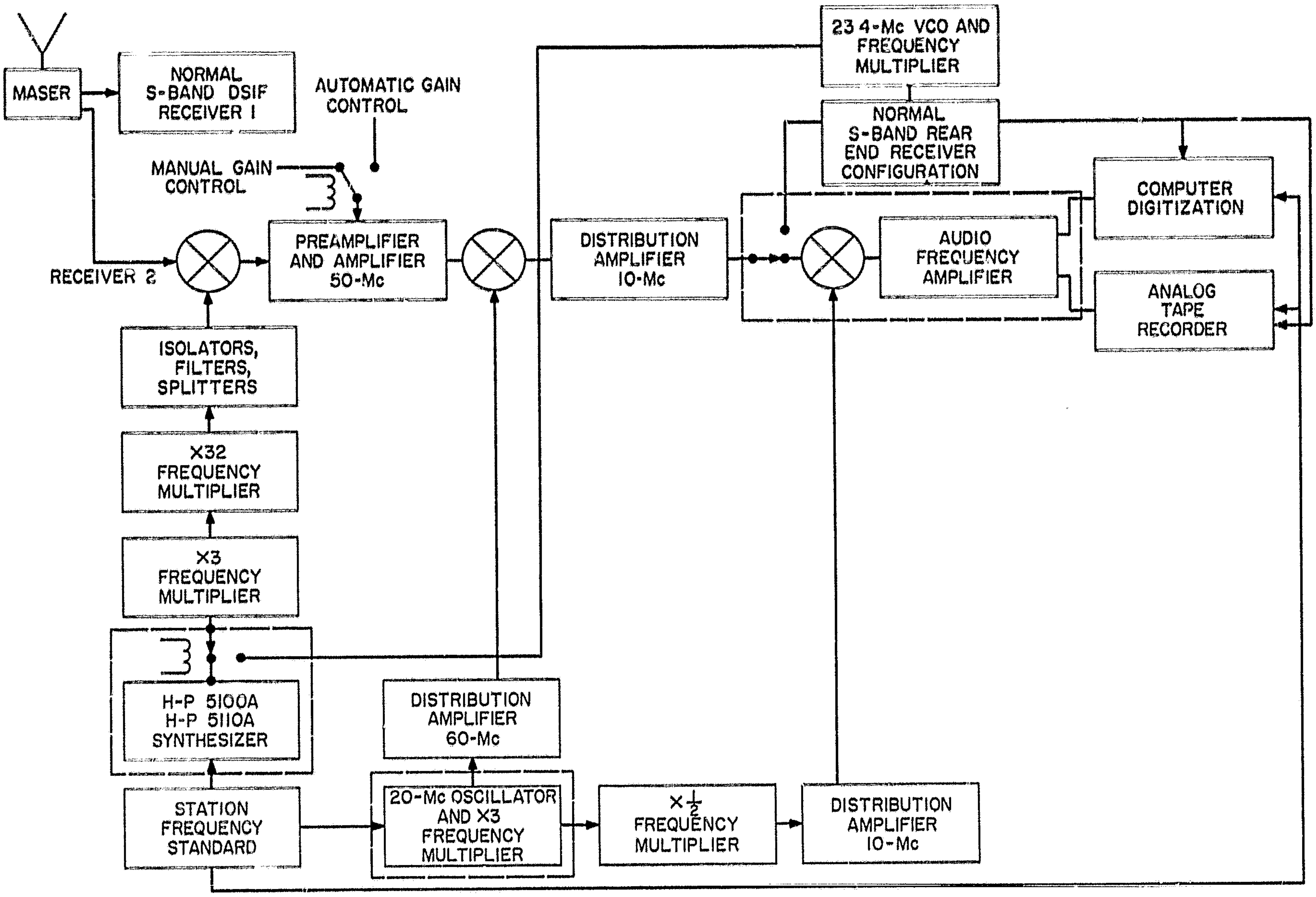

Fig. 5. Proposed receiver configuration for the *Mariner* C occultation experiment

because the second receiver channel can be used in its normal mode as a backup for the telemetry for all but a short period of time during the occultation experiment.

C. Advanced Antenna System

1. *Antenna Pedestal and Instrument Tower*

System performance of the Advanced Antenna System to its specified accuracy depends upon proper instrument tower and antenna pedestal foundation design and construction. The pedestal is constructed of mass-reinforced concrete and serves as a stable base for the antenna rotating elements; it transfers all vertical, horizontal, and rotational loads from the antenna through the pedestal foundation to the soil. As a secondary function, it houses service and operating areas. The general configuration of the pedestal is dictated by the foundation requirements, the primary reflector elevation range, and the local compliance requirements at the points of loading imposed by the alidade. A circular cutout is furnished in the center of the pedestal to accommodate the separate instrument tower. This tower provides a ground reference and support for the master equatorial mount for precision pointing command and angle data readout. The lower portion of the tower, to the top level of the pedestal, is concrete; the upper portion is steel.

The foundations of the pedestal and instrument tower are completely separate. Isolation is necessary to prevent antenna motion due to wind loads from causing a related motion of the instrument tower. (The tower is protected from the wind by a windshield on the alidade which completely surrounds it.) Any motion of the instrument tower would have an adverse effect on the accuracy of the tower as a pointing reference for the antenna reflector. In order to design the pedestal and instrument tower foundations to effect the necessary separation, detail soil studies were performed.

The antenna pedestal structure and the concrete portion of the instrument tower have been completed. Work is continuing on the interior of the pedestal, and installation of the steel portions of the tower will begin soon.

2. Alidade

The alidade is that portion of the antenna which rotates in azimuth and supports the tipping parts of the antenna in all attitudes and environmental conditions according to specified pointing requirements. The primary consideration in large high-frequency antenna design is maintaining a high degree of stiffness and, hence, small deflections in all structural elements. Once the required stiffness of the various members of the alidade structure was determined, it was necessary to fabricate a section to meet those requirements since no standard commercial steel sections were adequate. Several different configurations were studied. The section which best satisfied the design requirements was a composite section formed by welding four steel wide flange sections together in the configuration of a pentahedron space frame. The three base points are supported on hydrostatic bearing pads, and the two top points support the elevation bearings. The azimuth and elevation drives, receiving equipment, operating equipment rooms, instrument tower wind and thermal shield, and electrical substation are mounted on the alidade structure. On-site erection of the alidade is now in progress.

V. Space Flight Operations Facility

A. Introduction

The Space Flight Operations Facility (SFOF), located in a three-story building at JPL, utilizes operations control consoles, status and operations displays, computers, data-processing equipment for analysis of spacecraft performance and space science experiments, and communication facilities to control space flight operations. This control is accomplished by generating trajectories and orbits and command and control data from tracking and telemetry data received from the Deep Space Instrumentation Facility (DSIF) in near-real time. The SFOF also reduces the telemetry, tracking, command, and station performance data recorded by the DSIF into engineering and scientific information for analysis and use by the scientific experimenters and spacecraft engineers.

B. Special Power Supplies

The SFOF data-processing equipment and microwave equipment require a power source free of noise or other electrical transients. Switching surges, system faults, voltage drops, or power failure will cause deleterious effects to computer and microwave equipment operation. A special 300-kva power supply will be installed and operating in the SFOF by early 1965. This supply consists of a 400-hp, 550-v, 1800-rpm, dc motor driving a brushless, 4-salient-pole, 3-phase, revolving field-type generator coupled by a high-inertia flywheel. The motor is normally operated on commercial power supplied through an electronic bus. In the event of a commercial power failure, the motor will switch to a 300-cell lead–calcium standby battery bank, and a 625-kva emergency diesel motor generator will start. Once operating speed has been attained, this generator will be switched to the electronic bus. When ac power is restored to the electronic bus, either by the commercial power or by the emergency diesel generator, the battery bank will automatically be disconnected from the drive motor. Procedures and techniques for RFI control were incorporated in the basic design of the special power supply motor and generator in order that the amount of interference inherently generated and propagated would be restricted to a minimum.

The special power supply is backed up by a regulated supply. This backup will be employed during noncritical periods to perform routine maintenance on the special power supply.

The SFOF air-conditioning loads and other high transient loads are supplied by a separate commercial utility bus. In the event of a commercial power failure, a second emergency diesel motor generator will start automatically. This generator will be switched to the utility bus when operating speed is attained.